

UNIVERSITI TEKNOLOGI MALAYSIA

BORANG PENGESAHAN
LAPORAN AKHIR PENYELIDIKAN

TAJUK PROJEK : RF FRONT END DESIGN

Saya _ MOHAMAD KAMAL A RAHIM
(HURUF BESAR)

Mengaku membenarkan Laporan Akhir Penyelidikan ini disimpan di Perpustakaan Universiti Teknologi Malaysia dengan syarat-syarat kegunaan seperti berikut :

1. Laporan Akhir Penyelidikan ini adalah hakmilik Universiti Teknologi Malaysia.
2. Perpustakaan Universiti Teknologi Malaysia dibenarkan membuat salinan untuk tujuan rujukan sahaja.
3. Perpustakaan dibenarkan membuat penjualan salinan Laporan Akhir Penyelidikan ini bagi kategori TIDAK TERHAD.
4. * Sila tandakan (/)

☐

SULIT

(Mengandungi maklumat yang berdarjah keselamatan atau kepentingan Malaysia seperti yang termaktub di dalam AKTA RAHSIA RASMI 1972).

☐

TERHAD

(Mengandungi maklumat TERHAD yang telah ditentukan oleh Organisasi/badan di mana penyelidikan dijalankan).

☒

TIDAK
TERHAD

TANDATANGAN KETUA PENYELIDIK

MUHAMAD KAMAL B. ABD. RAHIM
PENSYARAH

FAKULTI KEJURUTERAAN ELEKTRIK
UNIVERSITI TEKNOLOGI MALAYSIA
KARUNG BERKUNCI 701.

~~MOHAMAD JOHARI RAHMAN~~
Nama & Cop Ketua Penyelidik

Tarikh : 6 APRIL 1999

CATATAN : * Jika Laporan Akhir Penyelidikan ini SULIT atau TERHAD, sila lampirkan surat daripada pihak berkuasa/organisasi berkenaan dengan menyatakan sekali sebab dan tempoh laporan ini perlu dikelaskan sebagai SULIT dan TERHAD.

ABSTRACT

Microstrip transmission line is used over the frequency range from 1 GHz to 40 GHz. The circuit dimensions at higher frequency are very small and circuit losses become high. In practice microstrip is used extensively over 2 to 12 GHz range where small compact circuits, suitable for the inclusion of active devices. The circuits using microstrip have several advantages such as light weight, small size, low cost as compared to conventional microwave waveguide. This project involves the design and fabrication of RF subsystems using microstrip line such as low pass filter, bandpass filter, power divider and hybrid line coupler. The performance of various design is analysed through simulation and measurement.

ABSTRAK

Talian penghantaran mikrojalur digunakan untuk frekuensi di antara 1 GHz hingga 40 GHz. Dimensi litar pada frekuensi tinggi adalah kecil dan kehilangan litar menjadi tinggi. Dalam praktik mikrojalur digunakan secara meluas pada julat di antara 2 hingga 12 GHz di mana litar yang kompleks dan kecil sesuai digunakan untuk memasukan peranti aktif. Litar menggunakan mikrojalur mempunyai beberapa kelebihan termasuk ringan, saiz kecil, harga murah dibandingkan pandugelombang untuk konvensional gelombang mikro. Projek ini terdiri dari reka bentuk subsistem RF menggunakan talian mikrojalur seperti penapis lulus rendah, penapis lulu jalur, pembahagi kuasa dan pengganding hybrid. Prestasi untuk rekabentuk di analisa menerusi penyelakuan dan pengukuran.

LIST OF CONTENTS

ABSTRACT	i
CONTENTS	ii

CONTENTS

CHAPTER	PAGES
1.0 INTRODUCTION	1
2.0 MICROSTRIP TRANSMISSION LINE	2
2.1 Introduction	2
2.2 Basic Microstrip	2
2.3 The Substrate	2
2.4 Metallization	3
2.5 Substrate Material	3
2.6 RT/DURIOD 5880	3
2.7 Dispersion	4
2.8 Discontinuities	6
2.9 Losses in microstrip	7
2.9.1 Conductor Loss	7
2.9.2 Dielectric Loss	8
2.9.3 Radiation Loss	9

2.10	Q-factor	10
2.11	Static-TEM Parameters	11
2.11.1	Propagation Modes	11
2.11.2	Characteristic Impedance Z_0	12
2.11.3	The Effective Permittivity ϵ_{eff}	13
2.11.4	Wavelength λ_g	13
3.0	RF SUBSYSTEM DESIGN USING MICROSTRIP TRANSMISSION LINE	15
3.1	Low Pass Filter Design	15
3.1.1	Scalling The Prototype Value	15
3.1.2	Microstrip Parameters	17
3.1.3	Specification	21
3.1.4	Designing The Circuit	22
3.1.5	Simulation and Optimization	23
3.2	Band Pass Filter Design	23
3.2.1	Introduction	23
3.2.2	Design Procedure for Mathematical Calculation	24
3.2.3	Bandpass Filter Specification	29
3.3	Band Stop Filter Design	30
3.3.1	Bandstop Filter Design Using Parallel Lines	31
3.3.2	Specification for Parallel Line Design	34
3.3.3	Bandstop Filter Design Using Open Circuited Stub	35
3.4	Wilkinson Power Divider Design	38
3.4.1	Synthesis Analysis	38

3.4.2 Design Specification	38
3.5 Branch Line Coupler Design	40
3.5.1 Microstrip Branch-line Coupler	41
4 RESULT, MEASUREMENT & SIMULATION	42
4.1 Measurement of Filters	42
4.1.1 Filters Measurement Result	44
4.1.2 Filters Simulation With PUFF	45
4.2 Measurement of Microstrip Branch-line Coupler	49
4.2.1 Result of The Measurements	50
4.3 Measurement and Analysis of Wilkinson Power Divider	54
4.3.1 Return Loss Measurement	54
4.3.2 Measurement Results for Wilkinson Power Divider	55
4.3.3 Design Analysis	56
5 DISCUSSION	58
5.1 Filters	58
5.2 Branch-line Coupler	59
5.3 Wilkinson Power Divider	59
6 CONCLUSION	62
REFERENCES	
APPENDIXES	

1.0 INTRODUCTION

The rapid development of wireless communications products over the last ten years has led to an explosion in interest in improved circuit design approaches in the radio frequency (RF) and microwave area. Microstrip circuits for microwave engineering have progressed through the research and development stages and are now found as integral part of many small-signal microwave systems.

Advanced development of microstrip technology has brought microstrip into a new era of communication world. Nowadays microstrip has become more and more popular and important as a communication in radio communication, satellite communication, cellular phone communications and other microwave transmission. In fact, microstrip technology reduced bulky conventional microwave components such as amplifier, oscillator, mixer, filter and detector. These lumped microwave components can be replaced by microstrip that acts as transmission lines that make microwave's components become miniature and lightweight.

Microstrip transmission lines has been discovered to be more efficient than other types of transmission lines like coaxial line, two-wired line and twisted-pair line. This mostly due to its lightweight and small sized with a similar or even better performance compared with those lines. Furthermore, microstrip transmission lines produced less loss and can be considered as a lossless transmission medium. However, microstrip transmission lines are not suitable for long distance transmission like connection from one place to another. It is design for small distance transmission for instance the transmission between two adjacent ports or terminals.

2.0 MICROSTRIP TRANSMISSION LINE

2.1 Introduction

Microstrips are printed circuit for very high frequency electronics and microwave. When made of conducting strips deposited upon a dielectric substrate, they are called microwave integrated circuits (MICs). Printed circuit are also made with semiconducting substrates, inside of which electronic devices (transistor, diodes) are fabricated by diffusion or ion implantation. The resulting structures are then called monolithic microwave integrated circuit (MMICs).

2.2 Basic Microstrip

Physically, any microstrip structure consists of a thin plate of low-loss insulating material, the substrate, covered with metal completely on one side, the ground plane, and partly on the other, where the circuit or antenna patterns are printed. Lumped components can be connected into the circuit (discrete components) or realized within the circuit (distributed components).

2.3 The Substrate

The substrate fulfills two functions:

1. It is a mechanical support that ensures that implanted components are properly positioned and mechanically stable, just as in printed circuits for low-frequency electronics.
2. It behaves as an integral part of connecting transmission lines and deposited circuit components: its permittivity and thickness determine the electrical characteristics of the circuit or antenna.

2.4 Metallization

Most commercially available microstrip substrates are metallized on both faces. The circuit pattern is realized by the photolithographic process. A mask of the circuit to be realized is drawn at a suitable scale, cut, and then reduced and placed on top of a photoresistive layer, which was previously deposited on top of the microstrip. The structure is then exposed to ultraviolet radiation, which reaches the photoresistive layers through the mask openings. The exposed parts are removed by the photographic development, and the metal cover is etched away from the exposed area. It is possible to deposit metal by evaporation or sputtering upon a bare dielectric substrate.

2.5 Substrate Material

Ideally a substrate should have very low-loss and constant dielectric properties over the range of frequencies for which it is used, together with excellent temperature and dimensional stability. In addition it should be chemically resistant, be easy to machine and provide a good thermal expansion match to the strip conductor material. For microwave application the value of ϵ_r dictates the size of the circuit. The substrate with permittivities ranging from 2.1 to 10 are readily available. Also important is the loss angle ($\tan \delta$) which gives a measure of the dielectric loss of the substrate.

2.6 RT/DUROID 5880

In this project, RT/DUROID 5880 is being chosen where it is a glass microfiber reinforced PTFE composite designed for exacting stripline and microstrip

applications. Glass reinforcing microfibers are randomly oriented to maximize benefits of the fiber reinforcement in the directions most valuable to circuit producers and in the final circuit application. The dielectric constant of RT/DUROID 5880 laminates is uniform from panel to panel and is constant over a wide frequency range. Its low dissipation factor extends the usefulness of RT/DUROID 5880 to X-band and above.

RT/DUROID 5880 laminates is easily cut, sheared and machined to shape. It has excellent dimensional stability and is resistant to all solvents and reagents, hot or cold, normally used in etching printed circuit or in plating edges and holes. When ordering RT/DUROID 5880 laminates, it is important to specify dielectric thickness, tolerance, rolled or electrodeposited copper foil, and weight of copper foil required.

Laminated microstrip – RT/DUROID 5880

(ROGERS) SERIAL NO.: 80310M104ACB

- DIELECTRIC CONSTANT, ϵ_r = 2.20 ± 0.02 (Relative Permittivity)
- MICROSTRIP HEIGHT, h = 0.031 ± 0.001 Inches
 0.78 ± 0.03 mm
- CLADDING (COPPER) = 35 μm Rolled or ED COPPER (loz)
- DISSIPATION FACTOR = 0.0009 typical

(At 10 GHz Nominal)

2.7 Dispersion

While non-TEM modes are not important as limiting factors for high-frequency operation of microstrip, they may cause dispersion at practical operating

frequencies. As more and more energy is transformed to surface waves, the effective dielectric constant will increase, resulting in a lower phase velocity. The dispersion will become stronger with increasing substrate thickness and dielectric constant.

The dispersion can be calculated numerically, but the calculation are very-time consuming and therefore costly. One method has been described by Getsinger, and his result confirm the above comments. They also show that in the useful operating frequency range of substrate with low dielectric constant, the dispersion is negligible. Getsinger⁽⁴⁾ has given simple formula for microstrip dispersion. He had obtained the functional relationship from calculation on a structure, which should similar dispersion. The resulting formula, with one undetermined constant, has then been fitted to experimental data for microstrip. The result is

$$\epsilon_{eff}(f) = \epsilon_r - \frac{\epsilon_r - \epsilon_{eff}}{1 + G \left(\frac{f}{f_p} \right)^2} \quad 2.1$$

Where ϵ_{eff} is the effective dielectric constant at zero frequency, G the undetermined constant, f the frequency and

$$f_p = \frac{Z_0}{2 \mu_0 h} \quad 2.2$$

The formula given by Getsinger for $G \approx 0.6 + 0.009Z_0$

For the same substrate thickness, dispersion will increase with the dielectric constant of the substrate. Thus, dispersion can safely be neglected for substrate with $\epsilon_r \approx 2 - 3$.

2.8 Discontinuities

Discontinuities in microstrip circuit are of eight basic groups :

- i. Foreshortened open circuit
- ii. Series coupling gap
- iii. Short circuit through to the ground plane
- iv. Right-angle corners or bend
- v. Step-width changes
- vi. Transverse slit
- vii. T-junction
- viii. Cross-junction

Discontinuities involves a change in dimension of the strip conductor giving rise to a change in electric and magnetic field distribution. This causes losses, reflection and radiation of energy.

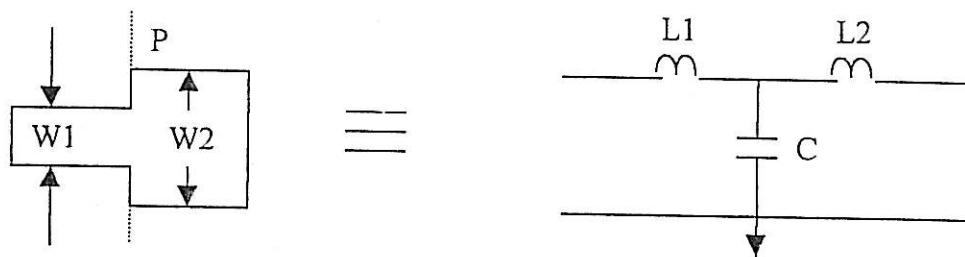


Figure 2.1 : Structure and equivalent circuit of the symmetrical microstrip step
(changes in width)

Steps in width exist at the junction of two microstrip lines having different impedance. The configuration for step discontinuity and its equivalent circuit is shown in fig 2.1. The step capacitances C_s have been given

$$\frac{C_s}{\sqrt{w_1 w_2}} = (10.1 \log \epsilon_r + 2.33) \frac{w_2}{w_1} - 12.6 \log \epsilon_r - 3.17 \quad 2.3$$

$$\epsilon_r \leq 10; 1.5 \leq \frac{w_2}{w_1} \leq 3.5$$

2.9 Losses in Microstrip

Microstrip transmission lines have had widespread use in microwave integrated circuits. For performing accurate circuit design, it is necessary to have adequate knowledge of the phase velocity, impedance and losses of four separate mechanisms :

- i. Conductor loss
- ii. Dielectric loss
- iii. Radiation loss

2.9.1 Conductor Loss

Loss due to finite conductivity in the strip and the ground plane can be calculated if the current distribution on the conductors are known. The current distribution can only be calculated numerically, making this method impractical for obtaining the general formula for the conductor losses. A rough approximation can be obtained by assuming uniform current distribution over the strip and the ground plane under the strip. These can be derived from the attenuation coefficient for loss lines,

$$\alpha_c = \frac{R}{2Z_0} \quad 2.4$$

where R is calculated taking the skin depth into account, i.e.

$$\alpha_c = \frac{0.072\sqrt{f}}{wZ_0} \text{ dB/unitlength- } f \text{ is in GHz.}$$

In practice this yield low results and surface roughness must be taken into account. The following empirical formula has been developed:

$$\alpha'_c = \alpha_c \left[1 + \frac{2}{\pi} \arctan \left(1.4 \left[\frac{\Delta}{\delta_s} \right]^2 \right) \right] \quad 2.5$$

Where $\delta_s = \frac{1}{\sigma R_s}$ skindepth, Δ = rms surface roughness, R_s = surface resistivity, σ = conductivity

2.9.2 Dielectric Loss

Dielectric loss in microstrip is usually much less than conductor loss except for poor quality substrates. The attenuation of a TEM wave due to dielectric loss is based on the attenuation constant. The dielectric attenuation factor is given by:

$$\alpha_d = 27.3 \frac{\epsilon_r (\epsilon_{eff} - 1) \tan \delta}{\sqrt{\epsilon_{eff}} (\epsilon_r - 1) \lambda_0} \text{ dB / unitlength} \quad 2.6$$

$$\text{Where, } \lambda_o = \lambda_g \sqrt{\epsilon_{eff}}$$

δ = loss tangent

2.9.3 Radiation Loss

In addition to the conductor and dielectric losses, microstrip line also has radiation losses. The radiation loss depends on the substrates, thickness and dielectric constant, as well as geometry. Lewin has calculated the radiation loss for several discontinuities using the following approximations :

- i. TEM transmission
- ii. Uniform dielectric in the neighborhood of the strip, equal in magnitude to an effective value.
- iii. Neglect of radiation from the transverse electric (TE) field component parallel to the strip.
- iv. Substrate thickness much less than free-space wavelength.

As microstrip is an open structure, power will be lost by radiation caused by any discontinuity in the strip. Radiation loss is proportional to $(h/\lambda_0)^2$, and the frequency at which certain substrate thickness can be used for a certain device or circuit will therefore have an upper limit, depending on the total amount of radiation that can tolerated (and the dielectric constant of the substrate). It can be represent as,

$$Y = G_r + G_s + jB \quad 2.7$$

Where,

G_r = conductance due to space-wave propagation

G_s = radiation conductance

B = susceptance

2.10 Q-factor

Many microwave integrated circuits require very high quality resonant circuits. The quality factor Q of a microstrip line is very high, but limited by the radiation losses of the substrate and with low dielectric constant.

Defining $Q = \omega_0 U / W$, where U is stored energy and W is the power lost per cycle and then⁽²⁾:

$$Q = \frac{\omega_0 (1/2 Li^2 + 1/2 CV^2)/2}{(Ri^2 + GV^2)/2} \quad \text{per unit length} \quad 2.8$$

But $V = IZ_0$ and then,

$$Q = \frac{\omega_0 (L/Z_0 + CZ_0)}{2(R/Z_0 + GZ_0)} \quad 2.9$$

Replacing Z_0 by $\sqrt{L/C}$ we obtain

$$Q = \frac{\omega_0 \sqrt{LC}}{R/Z_0 + GZ_0}$$

But $\omega_0 \sqrt{LC} = \beta$ and $\alpha = R/2Z_0 + GZ_0/Z$

And therefore

$$Q = \beta / 2\alpha$$

Finally $\beta \lambda g = 2\pi$ so

$$Q = \pi / \alpha \lambda g \quad \text{and}$$

$$\alpha = \pi / Q \lambda g \quad \text{nepers/meter}$$

and for a length l meter,

$$\alpha(l) = 8.686 \frac{\pi l}{Q \lambda g} \quad \text{dB} \quad 2.10$$

2.11 Static – Tem Parameters

There are many significant microstrip design calculation that require TEM-mode which result from transmission line theory. Below are some fundamental design parameters involved.

2.11.1 Propagation Modes

Any transmission system which is filled with a uniform will support a well defined mode propagation (TEM for coaxial lines, TE for waveguides). This is because the boundary conditions are relatively simple and can be satisfied by single wave types. A structure with a dielectric interface will not support a single propagation mode because of the added boundary conditions at the dielectric interface. Gupta⁽⁵⁾ have shown that longitudinal electric and magnetic components are also present. Fortunately the majority of the transmitted energy is propagated in a field distribution with closely resembles a TEM mode and is referred to as a quasi TEM. A typical distribution of the field is shown in figure 2.5.1. Note hoe the E field is spreads out in the dielectric material because $\epsilon_r > 1$. This effects the amount of coupling between two adjacent lines.

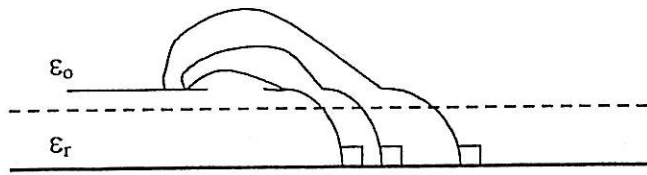


Figure 2.2 : A typical distribution of the field

2.11.2 Characteristic Impedance Z_0

For a microstrip geometry the impedance to TEM wave will be of the form⁽²⁾:

$$Z_0 = \sqrt{\frac{L}{C}} \quad 2.11$$

The phase velocity V_p of the wave travelling along the line is given by,

$$V_p = \frac{1}{\sqrt{LC}} \quad 2.12$$

If the dielectric substrate could be removed leaving air-spaced line of the same geometry (velocity of light in free-space $c = 2.99393 \times 10^8 \text{ ms}^{-1}$), its characteristic impedance Z_{01} would be,

$$Z_{01} = \sqrt{\frac{L}{C_1}} \quad 2.13$$

$$Z_{01} = cL \quad 2.14$$

$$Z_{01} = \frac{1}{cC_1} \quad 2.15$$

Where L is inductance, C is capacitance and C_1 is the capacitance per unit length this structure. Eliminating the equation 2.13, 2.14 and 2.15 gives,

$$Z_0 = \frac{1}{c\sqrt{CC_1}} \quad 2.16$$

2.11.3 The Effective Permittivity (ϵ_{eff})

The velocity in the microstrip is $v = \frac{1}{\sqrt{LC}}$ 2.17

and in the equipment air line $c = \frac{1}{\sqrt{LC_1}}$ 2.18

from which it is seen that,

$$v = \frac{c}{\sqrt{\epsilon_{eff}}} = \frac{c}{\sqrt{\frac{C}{C_1}}} \quad 2.19 \quad \text{and therefore}$$

$$\epsilon_{eff} = \frac{C}{C_1} = \left(\frac{c}{V_p} \right)^2 \quad 2.20$$

The characteristic impedance of the microstrip can then expressed as

$$Z_{01} = Z_0 \sqrt{\epsilon_{eff}} \quad 2.21$$

This important result. It states that the characteristic impedance of a microstrip can be determined in terms of the Z_0 of an equivalent air line (with simple boundary condition) and an effective permeability.

2.11.4 Wavelength (λ_g)

The synthesis regarding a single line and parallel lines need different approach where the latter involves with extensive calculations. Depended on the single line

microstrip, we know that $\epsilon_{eff} = (c/v_p)^2$. For free space $c = f\lambda_0$ and in microstrip

$v_p = f\lambda_g$ substitute into $\epsilon_{eff} = (c/v_p)^2$ and giving (2),

$$\epsilon_{eff} = \left(\frac{\lambda_0}{\lambda_g} \right)^2 \quad 2.22$$

$$\text{thus } \lambda_g = \frac{\lambda_0}{\sqrt{\epsilon_{eff}}} \quad 2.23$$

in F gigahertz and λ_g millimetre

$$\lambda_g = \frac{300}{F\sqrt{\epsilon_{eff}}} \text{ mm} \quad 2.24$$

3.0 RF SUBSYSTEM DESIGN USING MICROSTRIP TRANSMISSION LINE.

3.1 Low Pass Filter Design.

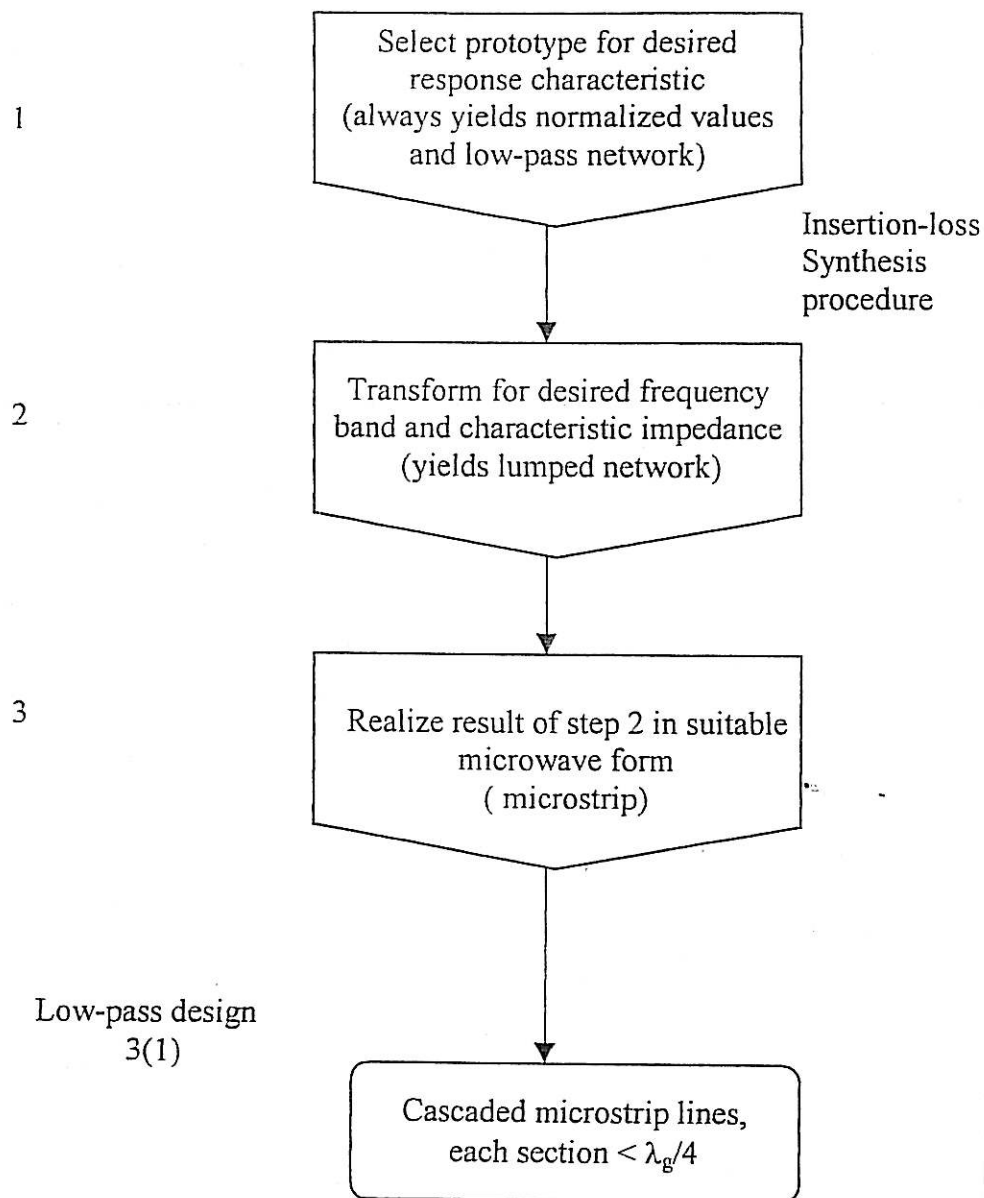
Table 3.1 shows the typical sequence which starts with a prototype specification and finishes with a practical, fully dimensioned and microstrip circuit. For this design we shall employ cascaded section of the microstrip as indicated by step 3 (1) of the Table 3.1, although this technique is only really useful at frequencies up to several gigahertz. It is first necessary to analyse the direct substitution of the lumped filter elements such as microstrip length.

3.1.1 Scaling The Prototype Values

When specify the filter, choose the appropriate attenuation response, and write down the low-pass prototype values and the next step is transform the prototype circuit into usable filter. After that make sure the cut-off frequency of the prototype circuit is 0.159 Hz ($\omega = 1$ rad/sec), and it operates between a source and load resistance that normalized so that $R_L = 1$ ohm. The transformation is affected the following formulas⁽¹⁾:

$$C = \frac{C_n}{2\pi f_c} \quad \text{and} \quad L = RL_n / 2\pi f_c \quad 3.1$$

Table 3.1 :Low-pass filter design procedure



Low-pass design
3(1)

Where

C – the final capacitor value

L – the final inductor value

C_n – a low-pass prototype element value

L_n – a low-pass prototype element value

R – the final load resistor

F_c – the final cut-off frequency

The normalized low-pass prototype source resistor must also transformed to its final value of the load resistor. Thus the ratio of the always remain the same. The detail steps for designing the low-pass prototype filter are mentioned below:

1. Define the response by specifying the required attenuation characteristics at selected frequencies.
2. Normalize the frequencies of the interest by dividing them by the cut-off frequency of filter. The step forces your data to be in the same form as that of the attenuation curves, the 3 dB point on the curve is:

$$f_{att} / f_c = 1$$

3. Determine the maximum amount of ripple that can allow in the pass band. Remember the greater the amount of ripple allowed, the more selective the filter is. Higher values of the ripple may allow to eliminate a few components.
4. Match the normalized attenuation characteristic (step 1 and 2) with the attenuation curves. Allow a small “fudge-factor” for good measure. This step reveals the minimum number of circuit element that can bet away with-given the certain filter type.
5. Scale all the elements to the frequency and impedance of final design.

3.1.2 The Microstrip Parameter

Consider a practical low-pass filter with alternating high and low impedance sections. There will be fringing fields from the ends of the low impedance line. Let us first consider a predominantly inductance given by⁽³⁾,

$$l_L = \frac{\lambda_{gL}}{2\pi} \sin^{-1} \left[\frac{2\pi fL}{Z_{oL}} \right] \quad 3.2$$

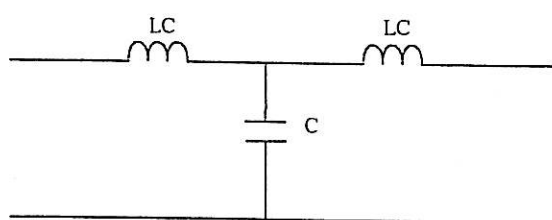
With the two shunt-capacitance elements

$$C_L = \frac{1}{2\pi fZ_{oL}} \tan \left[\frac{\pi l_L}{\lambda_{gL}} \right] \quad 3.3$$

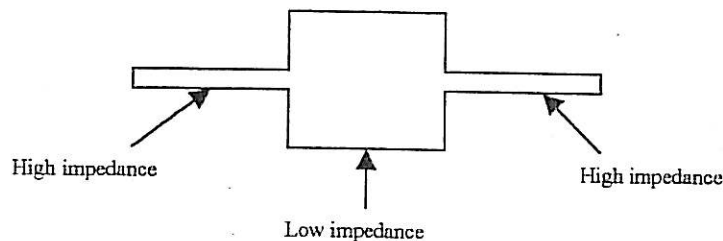
Where,

λ_{gL} – the wavelength associated with the high impedance microstrip line

Z_{oL} – the characteristic impedance associated with the high impedance microstrip line.



(i) Lumped equivalent



(ii) Microstrip form

Figure 3.1 : Inductive length of line with adjacent capacitive line

The figure 3.1 shows that the inductive length of line l with adjacent lengths of low impedance (capacitive lines) and therefore, wide microstrip lines.

In a similar manner for the low impedance line, the line of length for the desired capacitance is given by,

$$l_c = \frac{\lambda_{gc}}{2\pi} \sin^{-1} [2\pi f C Z_{oc}] \quad 3.4$$

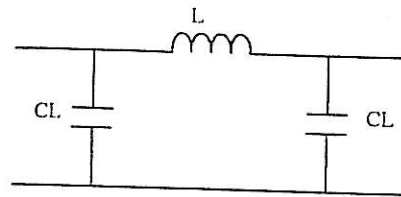
And the two series-inductance elements of the T-equivalent model are

$$L_c = \frac{Z_{oc}}{2\pi f} \tan \left[\frac{\pi l_c}{\lambda_{gL}} \right] \quad 3.5$$

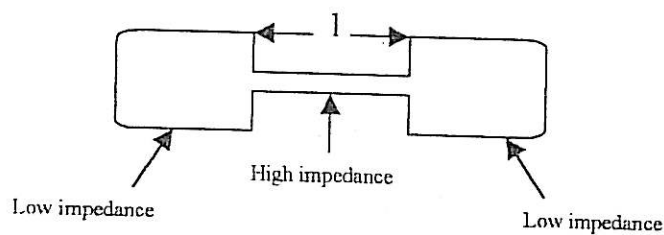
Where,

λ_{gL} – the wavelength associated with the low impedance microstrip line

Z_{oc} – the characteristic impedance associated with the low impedance microstrip line.



(i) Lumped circuit



(ii) Microstrip form

Figure 3.2 : Capacitive length of line with adjacent inductive lines

The transmission line lengths of practical low-pass filter are around using an interactive procedure.

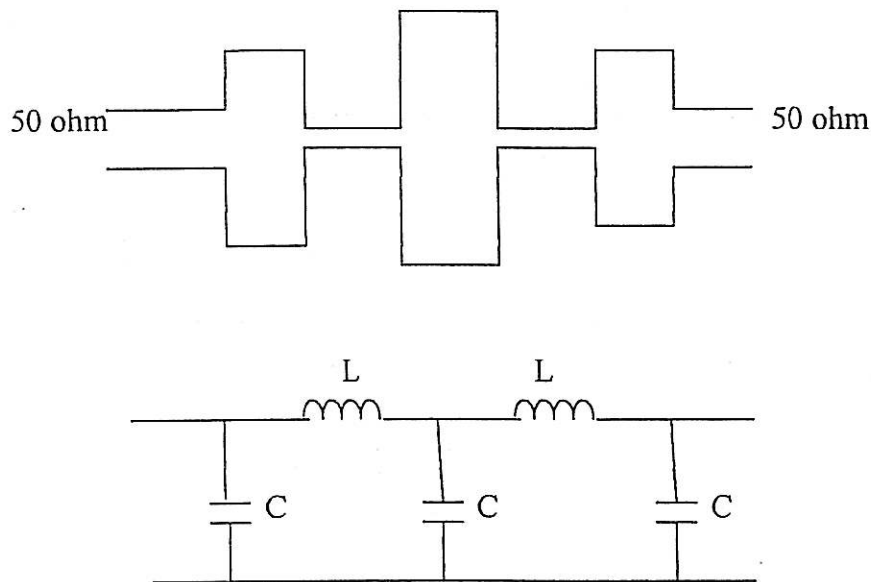


Figure 3.3 : Complete 5 element low pass filter

The filter is the equivalent of a 5 element L-C ladder network. The L and C values are designed to produce the required cut-off frequency, the frequency determining the limit of the pass band range and the rate at which the loss rises in the attenuation band.

The series inductance L elements are synthesised using short lengths of high impedance lines as indicated in fig. 3.1. The characteristic impedance of a microstrip line is a function of its width w ; the smaller w the higher the impedance. The shunt capacitance C elements are synthesised again by short lengths but of relatively large w to give the line a low characteristic impedance. Short lengths of low impedance line terminated in high impedance lines simulate closely a shunt capacitance as indicated in fig 3.2.

In complete filter fig. 3.3, corrections must be made for the abrupt junction discontinuities between adjacent elements and the effects of terminations on the L and C line elements. In practice microstrip filters are designed using computer aided design packages which accurately model all these effects and also contain facilities for simulated testing and optimisation. In this way the L and C line lengths and respective widths can be obtained with good degree of confidence that they satisfy the filter specification before fabrication is commenced.

3.1.3 Specification

The specification for the low-pass filter are as following :

- | | | |
|--|---|-----------------------|
| 1. Operating frequency (cut-off frequency) | = | 2.1 GHz |
| 2. Insertion Loss | = | <-0.5 |
| 3. VSWR | = | < 1.5 |
| 4. Ripple | = | 0.5 dB |
| 5. Attenuation for all frequencies above 3 GHz | = | 28 dB (out of band) |
| 6. Type of filter | = | Chebyshev filter |

The required specification are shown in figure 4.4. The cut-off frequency f_c (3 dB down) for the low-pass filter are chosen to be at 2.1 GHz. The minimum requirement of attenuation is 28 dB at 3 GHz.

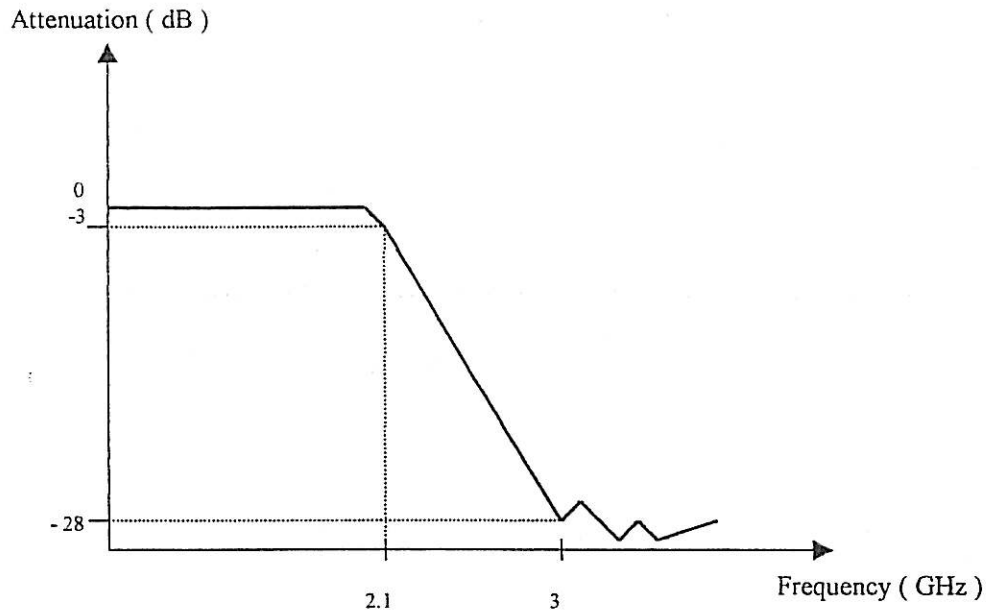


Figure 3.4 : The required low-pass filter response

3.1.4 Designing The Circuit

Let us further assume that a suitable prototype has been selected, to meet this specification and that the transformed, lumped low-pass filter network has been calculated. For a fifth-order Chebyshev filter, the element values of each section is given in table 3.5. Some prior design information must be provided about the microstrip lines, because expressions for inductance and capacitance depend upon both characteristic impedance and length. It is reasonable to initially fix the characteristic impedance because their orders of magnitude are roughly prescribed according to :

- i. $Z_{oc} \text{ (capacitance)} < Z_0 \text{ (50 ohm)} \ll Z_{oL} \text{ (inductance)}$

- ii. Z_{oL} must not be so large that its manufacture becomes inordinately difficult as a narrow line or its current-carrying capability becomes a limitation. In this case the values given below are reasonable starting values of impedance :

Capacitance lines : $Z_{oc} = 20 \text{ ohm}$

Inductive lines : $Z_{oL} = 90 \text{ ohm}$

3.1.5 Simulation and Optimization

In this project, the simulation and optimization of the microstrip low-pass filter is done by using a software called PUFF which is a computer aided design for microwave integrated circuits. PUFF is a scattering parameter and layout calculator for microwave circuits. It was created as an inexpensive and simple-to-use alternative to professional software whose high cost, copy protection schemes and training requirements create difficulties in academic environment.

PUFF uses a circuit laid out on the screen using cursor keys, a frequency or time domain analysis is available with a few keystrokes. It uses a simple heuristic format. The layout that is created on the puff screen is scale replica of the circuit. The parameters that can be obtained from the PUFF are: S_{11} (return loss), S_{12} (insertion loss), S_{21} , S_{22} , Smith chart response and the design layout. The advantage of using PUFF is that theoretical design can improved by simulating the design and modify to get the best design. If desired, the simulation also can be optimized to meet the desired specification.

3.2 Band Pass Filter Design

3.2.1 Introduction

In this chapter the design procedures of the band pass filter using the parallel-coupled microstrip lines will be discussed. Generally, the design process is divided into two categories, that are :

- Mathematical calculations
- Simulation with PUFF

The final result of the design process is obtained after doing some manual optimisation in PUFF by doing some adjustments to the TEM-parameters in order to meet the best design requirements.

3.2.2 Design Procedures For Mathematical Calculation

The main design steps are as follows :

1. Mapping from low-pass prototype to band pass.
2. Determine number of resonators, that is the order of the filter.
3. Calculate admittance inverters values.
4. Evaluate the even and odd mode characteristic impedance (Z_{oe} and Z_{oo}).
5. Calculate the value of resonators width (w) and separation (s).
6. Calculate the resonators length.
7. Simulate with CAD package – PUFF
8. Analysis and optimisation.

The design steps is done according to the method shown by Terry Edwards in his book 'Foundations for Microstrip Circuit Design'. The recommended steps are very systematic and easy to apply.

Step 1

Designing process starts with the transformation of low pass prototype into band pass requirement. The purpose of this idea is to determined the number of resonators that is needed to meet the attenuation requirement. This is to determine the order of the filter. The mapping of low pass prototype into band pass is done by using the

equation below :

$$\frac{\omega_i}{\omega_c} = \frac{2}{\delta} \left(\frac{f_i - f_0}{f_0} \right) \quad 3.6$$

where

$$\delta = \frac{f_2 - f_1}{f_0} \quad 3.7$$

δ = fractional bandwidth

f_1 = lower pass band

f_2 = upper pass band

f_0 = center frequency

ω_c = prototype cut-off frequency (equals to 1.0)

ω_i = defined at filter specification (started at early stage)

f_i = frequency at desired attenuation

The characteristic of a insertion loss characteristic response for bandpass filter is shown in figure 3.6

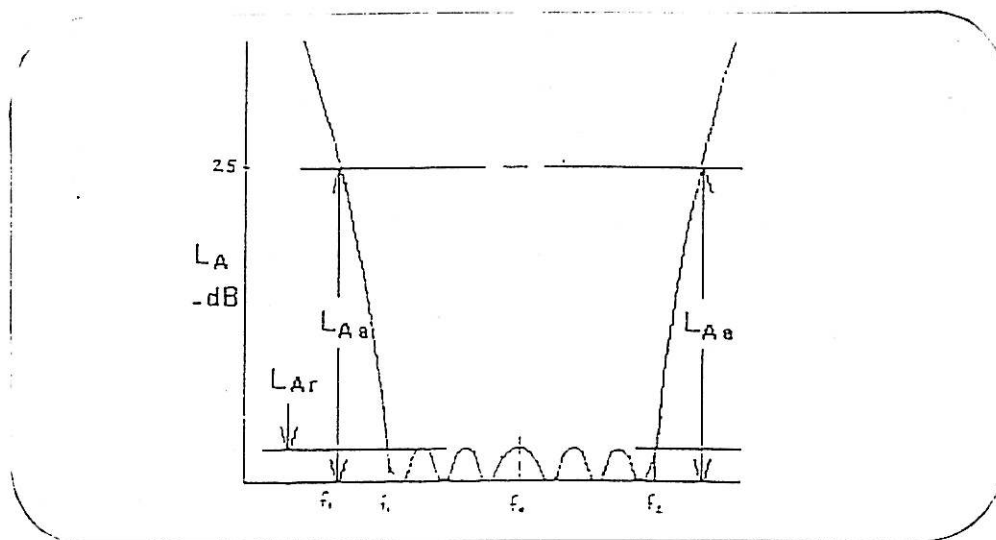


Figure 3.6 : Desired filter response

Step 2

Determine the order of the filter that is the value for 'n', by examining the filter prototype specifications which meet the insertion loss requirements, that is should be at least 20 dB (desired attenuation) for the desired frequency in the design specifications. For n^{th} -order of filter there will be $n+1$ number of resonators (coupled region). The order of the filter is determined by referring the graph for Chebyshev characteristic for 0.01 ripple. This graph is provided by G.Matthaei, L.Young and E.M.T Jones in their book 'Microwave Filter, Impedance Matching Networks and Coupling Structure'.

Step 3

A network consisting of admittance inverters and uniform-type resonant circuits were used. The admittance inverter parameters are then calculated.

For the first coupling structure
$$\frac{J_{01}}{Y_0} = \sqrt{\frac{\pi\delta}{2g_0g_1}} \quad 3.8$$

For intermediate coupling structures
$$\frac{J_{j,j+1}}{Y_0} \Big|_{j=1 \text{ to } (n-1)} = \frac{\pi\delta}{2\omega_c \sqrt{g_j g_{j+1}}} \quad 3.9$$

For the final coupling structure
$$\frac{J_{n,n+1}}{Y_0} = \sqrt{\frac{\pi\delta}{2g_n g_{n+1}}} \quad 3.10$$

The quantities 'g' refer to the prototype elements value which is readily available from the table provided in the book by G. Matthaei and groups. The value for 'g' is selected according to the order $2n+1$ of the filter.

Step 4

The odd-mode and even mode coupled line impedances Z_{0o} and Z_{0e} are then calculated by using the formula :

$$(Z_{0e})_{j,j+1} = Z_0 (1 + aZ_0 + a^2 Z_0^2) \quad 3.11$$

and
$$(Z_{0e})_{j,j+1} = Z_0 (1 + aZ_0 + a^2 Z_0^2) \quad 3.12$$

where $a = J_{j,j+1}$

Z_0 = system characteristic impedance (usually 50Ω)

Step 5

The microstrip line dimensions are finally obtained as follows. The width (w) and separation (s) with relation to odd and even mode characteristic impedances is evaluated by using equation below

$$\frac{w}{h} = \left(\frac{\exp H'}{8} - \frac{1}{4 \exp H'} \right) \quad 3.13$$

where
$$H' = \frac{Z_0 \sqrt{2(\epsilon_r + 1)}}{119.9} + \frac{1(\epsilon_r - 1)}{2(\epsilon_r + 1)} \left(\ln \frac{\pi}{2} + \frac{1}{\epsilon_r} \ln 4 \right) \quad 3.14$$

Using Akhtarzab et al. Synthesis : For $(w/h)_{se}$
$$Z_0 = \frac{Z_{0e}}{2} \quad 3.15$$

For $(w/h)_{so}$
$$Z_0 = \frac{Z_{0o}}{2} \quad 3.16$$

The value of s , that is the separation can be calculated by :

$$\frac{s}{h} = \frac{2}{\pi} \cosh^{-1} + \left[\frac{\cosh(\pi/2)(w/h)_{se} + \cosh(\pi/2)(w/h)_{so} - 2}{\cosh(\pi/2)(w/h)_{so} + \cosh(\pi/2)(w/h)_{se}} \right] \quad 3.17$$

However, in this project, we are not calculating manually the dimensions for the width (w) and separation (s). the final determination of these values (for fully manual calculation) will need some approximation method by using the general curves by Akhtarzad et al. This curves is attached in Appendix C. in this project the results for these dimensions are obtained from PUFF simulation.

Step 6

The length of the resonator is calculated by using equation below where we

have to evaluate :
$$\lambda_g = \frac{300}{F \sqrt{\epsilon_{eff}}} \quad 3.18$$

- The physical length of the resonators is $\lambda_g/2$
- The physical value of the coupled region is $\lambda_g/4$

In order to compensate the fringing effect, microstrip line is shortened by d where the value of d can be evaluated by equation 3.19. The fringing effect has to be

considered in the fabrication process. In PUFF simulation model this effect is

neglected. $Q = \frac{f_c}{f_2 - f_1}$ 3.19

3.2.3 Bandpass filter specification

The substrate used to design is RT Duriod 5880. The specification for the filter is:

$$Z_0 = 50\Omega$$

$$h = 0.510\text{mm}$$

Values of the parameters for chosen substrate.

$$\epsilon_r = 2.20$$

$$f_0 = 2.0 \text{ GHz}$$

$$f_1 = 1.9\text{GHz}$$

$$f_2 = 2.1\text{GHz}$$

$$\Delta f = f_2 - f_1 = 0.2\text{GHz}$$

$$\text{Response selected} : \text{Chebyshev}$$

$$\text{Attenuation} : >20\text{dB insertion loss}$$

$$\text{Ripple} : 0.01 \text{ dB}$$

$$f_i = f_3 : 1.7 \text{ GHz (assumed value at 20 dB)}$$

where

$$f_i = \text{frequency at desired attenuation, in this case at 20 dB}$$

$$f_0 = \text{centre frequency}$$

$$f_1 = \text{lower frequency at 3 dB}$$

$$f_2 = \text{upper frequency at 3 dB}$$

$$\Delta f = \text{bandwidth}$$

The fractional bandwidth : $\delta = \frac{2.1-1.9}{2.0} = 0.1$

The transformation from low pass to band pass filter is: $\frac{\omega_i'}{\omega_c} = \frac{2}{\delta} \left(\frac{f_i - f_0}{f_0} \right)$

$$= \frac{2}{0.1} \left(\frac{1.7 - 2.0}{2.0} \right) = -3$$

Now consider the Chebyshev graph for prototype filter insertion loss characteristic for pass band ripple of 0.01 dB, this is attached in Appendix .

$$\left| \frac{\omega_i'}{\omega_c} \right| - 1 = |-3| - 1 = 2$$

From the Chebyshev graph, $n = 4$ gives attenuation more than 20 dB, as the requirement for the design. So a fourth order band pass is being designed.

3.3 Band Stop Filter Design

In this chapter the design procedures of the band stop filter will be discussed.

The designed of band stop filter that will be discussed is;

- (a) band stop filter using parallel line and
- (b) band stop filter using open circuited stubs.

Generally, the designed process is divided into two categories, that are :

- (1) Mathematical calculations
- (2) Simulation with PUFF

The final result of the design process is obtained after doing some manual optimization in PUFF by doing some adjustments to the TEM-parameters in order to

meet the best design requirements. The designed finally will be fabricated refer to the result of the designed process. The substrate use for fabricate is RT Duroid 5880.

3.3.1 Bandstop Filters Design Using Parallel Lines

• Step 1

Designing process starts with the transformation of low-pass prototype into band-stop requirement. The bandstop characteristic function is given in the case of the Butterworth approximation problem in the θ -plane by

$$K(\theta^2) = \left(\frac{\Omega}{\Omega_c} \right)^{2n} \quad 3.20$$

$$\text{where } j\Omega = j \tan \theta \quad 3.21$$

$$j\Omega_c = j \tan \theta_c \quad 3.22$$

The frequency response of the circuit is

$$\theta = \frac{\pi}{2} \left(\frac{\omega}{\omega_0} \right) \quad 3.23$$

$$\theta_c = \frac{\pi}{2} \left(\frac{\omega_c}{\omega_0} \right) \quad 3.24$$

where $\omega_0 =$ mid-band edge

$\omega_c =$ upper-band edge

$\omega =$ radian

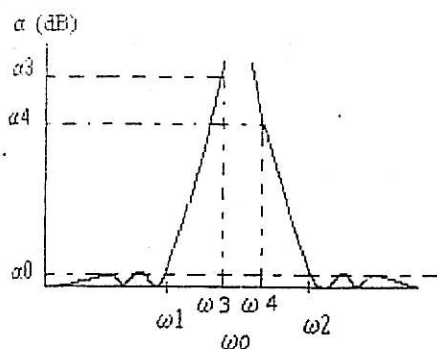


Figure 3.7 : Frequency Response of Bandstop filter

Step 2

Determine the number n of resonators used in the band-stop filter structure (which is equal to the number of reactive elements in the low-pass prototype). The number n of resonator is equal to the peaks of attenuation at ω_0 , $3\omega_0$, etc, each have a multiple-order pole of attenuation.

The design of the Butterworth filter is complete once its degree is specified. This quantity is fixed by the definition of its lower and upper band edge:

$$n = \frac{\log_{10} (A - 1)}{2 \log_{10} (\Omega_1 / \Omega_c)} \quad 3.25$$

where $A = 10^{a/10}$ 3.26

where $\Omega_c =$ upper-band edge

$\Omega_1 =$ frequency at which the attenuation is stopband

The degree of the equal ripple solution is fixed by the attenuation α_1 at Ω_1 in the stop band.

Step 3

The required development in the case of the parallel line topology now be illustrated for the degree-3 network in figure 3.8

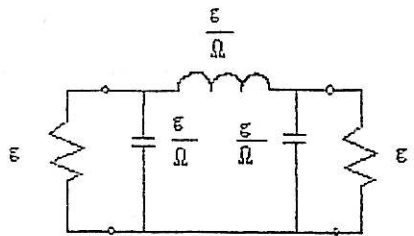


Figure 3.8: Degree-3 Bandstop Ladder Network

The entries of the ladder network are defined by $\frac{g_1}{\Omega_c}, \frac{g_2}{\Omega_c}, \frac{g_3}{\Omega_c}$

with $g_0 = g_4 = 1$.

The quantities of 'g' refer to prototype elements value which is readily available from the table provide in the book by G.Matthaei and groups. The value of 'g' is selected according to the order 'n' of the filter. Some of the prototype element values are listed in and shown in Appendix C.

Step 5

The dimensions of the parallel line circuit where we have to evaluate is;

- 1) the physical length of the resonator is $\lambda_g/2$ and
- 2) the physical value of the couple region is $\lambda_g/4$.

The fringing effect has to be considered in fabrication process. In PUFF simulation model, this effect is neglected.

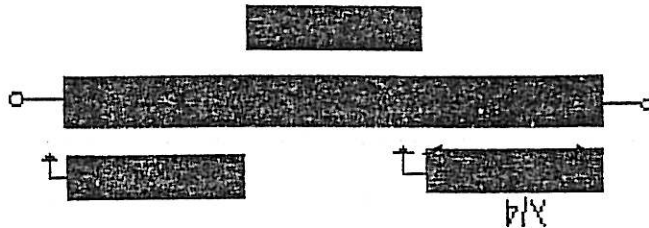


Figure 3.9 : Degree-3 Bandstop Filter Using Pairs of Parallel Line

3.3.2 Specification for Parallel Line Design

The substrate to design is RT Duroid 5880. The specification for the substrate is attached in Appendix C. the specification for the filter is:

- Cut-off frequency, f_0 = 2.0 GHz
- Attenuation = >20 dB
- Ripple = 0.01 dB
- Characteristic impedance, Z_0 = 50 Ω
- Substrate relative permittivity, ϵ_r = 2.2
- Substrate thickness, h = 0.79 mm

3.3.3 Bandstop Filter Design Using Open Circuited Stub

- Step 1

Designing process starts with the transformation of low-pass prototype into bandstop requirement. The purpose of designing bandstop filter from low-pass prototype, it is quite easy to compute the effect of finite resonator on the maximum stop band attenuation. The relationship of the low-pass prototype response to that of the basic transmission line filter is illustrated in figure 3.10 (a) and figure 3.10 (b)

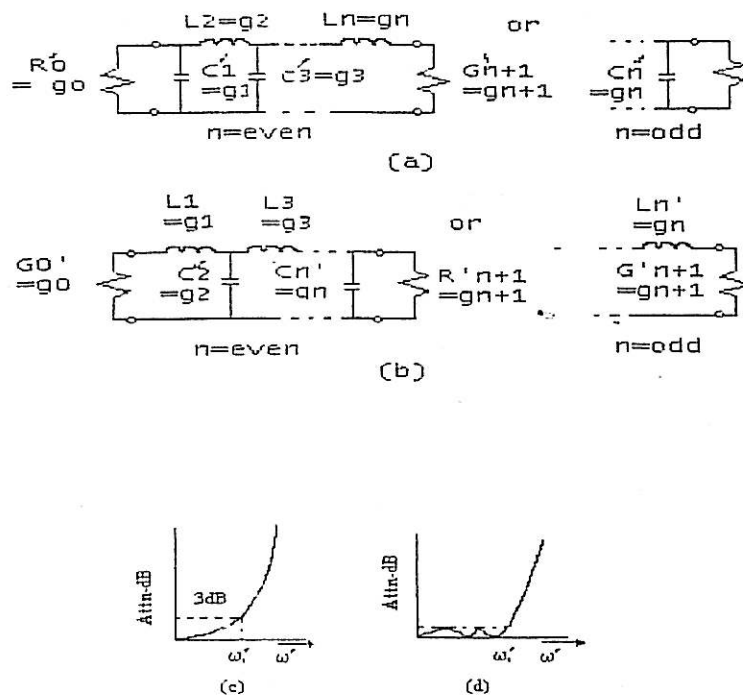


Figure 3.10 (a) : Low pass prototype (i), (ii) Four basic circuit types defining the parameter g_0, g_1, \dots, g_{n+1} (ii), (iv) Maximally flat and equiripple characteristic defining the band edge ω_1'

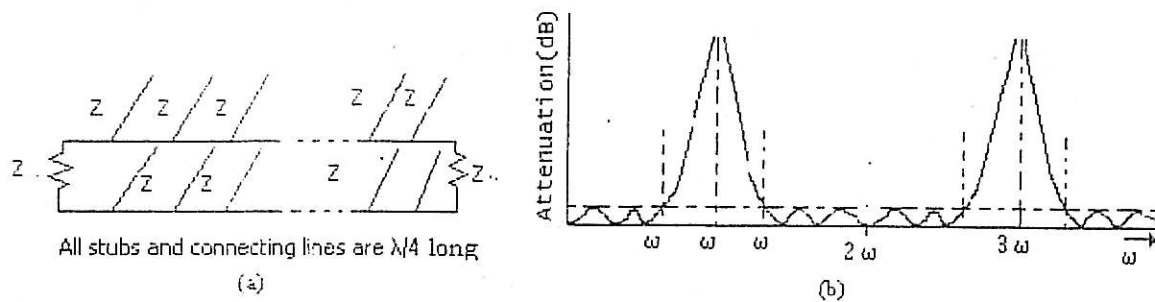


Figure 3.10 (b) : Bandstop filter (i) n-stub transmission line filter derived from n-element low pass prototype; (ii) equiripple characteristic defining center frequency ω_0 , parameter a , and stop band fractional bandwidth w

- Step 2

Determine the number n of resonators are used in the band-stop filter structure (which is equal to the number of reactive elements in the low-pass prototype). The number n of resonator is equal to the peaks of attenuation at ω_0 , $3\omega_0$, etc., each have a multiple-order pole of attenuation. The characteristic defining center frequency ω_0 , parameter α and stop band fractional band width is shown on figure 3.10(a).

- Step 3

The prototype network of figure 3.10 (a) to the transmission line network of figure 3.10 (b) are given as Step 4. The number of stub chosen to design bandstop filter is; $n = 3$. The prototype element values (obtained from table 4.05-2 (a) Matthaei, young and jones) show in Appendix C. the specification of those filter is:

- Cut-off frequency = 2 GHz
- Input Impedance = 50 Hz
- Ripple = 0.1 dB passband

- Stop band bandwidth = 60 per cent

The design of open circuit stubs band stop filter show in figure 5.8 can be

calculate by using the formula below. $Z_1 = \frac{Z_A}{Ag_0g_1}$ 3.27

$$Z_2 = \frac{Z_A g_0}{Ag_2} \quad 3.28$$

$$Z_3 = \frac{Z_A g_0}{g_4} \left(1 + \frac{1}{Ag_3g_4} \right) \quad 3.29$$

$$Z_{12} = Z_A (1 + Ag_0g_1) \quad 3.30$$

$$Z_{23} = \frac{Z_A g_0}{g_4} (1 + Ag_3g_4) \quad 3.31$$

The source impedance (Z_A) using is 50Ω and the right hand terminating impedance (Z_B) is also 50Ω .

• Step 5

The dimension of the design in figure 3.11 is refer to $\lambda/4$ long each stub. The length of the stub is depend on the value of the impedance. This parameter also can be visualized by using PUFF.

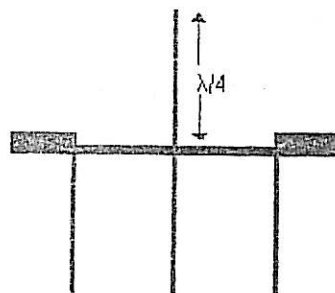


Figure 3.11: Design of open circuit stubs bandstop filter ($n=3$)

3.4 Wilkinson Power Divider design

In this project , 2 types of Wilkinson Power Divider are designed, which consists of uncompensated and compensated divider. The shape that being considered are mitered and radial bend microstrip power divider. Basically, to begin the design synthesis analysis must be considered.

3.4.1 Synthesis analysis

The synthesis analysis is closed formula to derive the characteristic impedance and propagation coefficient for a microstrip transmission line. The design of transmission line, it is necessary to derive w/h for a specific value of the characteristic impedance, assuming the substrate permittivity is known. Therefore, the analysis is for determine the w and ϵ_{eff} .

3.4.2 Design specification

Operating frequency	1 – 3 GHz
Center frequency	2 GHz
Coupling	3 dB
VSWR	< 1.60
Return Loss at each port	> -18 dB

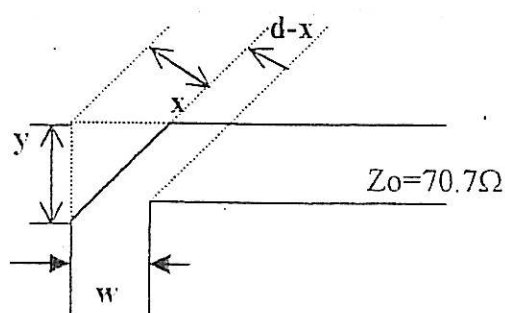


Figure 3.12: Compensation technique for uncompensated Power Divider

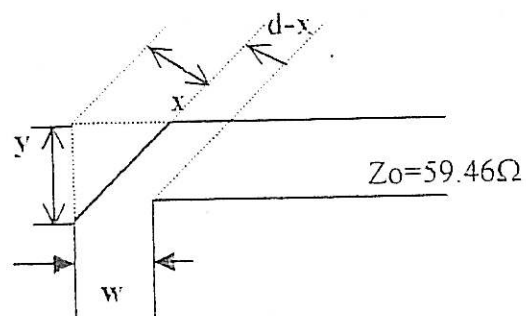


Figure 3.13 : Compensation technique for Compensated Power Divider

Finally, for compensated power divider, need to compensate the symmetrical step. It is located between quarter wave transformer and input port.

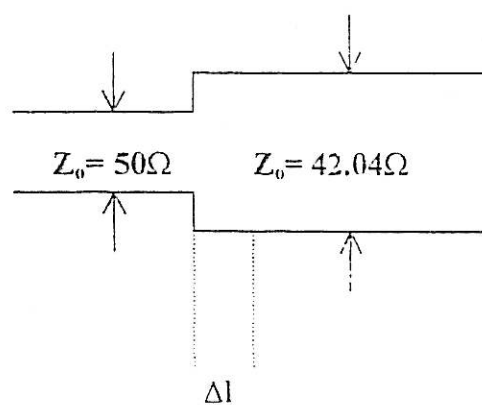


Figure 3.14 : Compensation technique for symmetrical step for compensated Power divider

3.5 Branch Line Coupler Design

This technique determines the shape ratio, w/h and s/h from Z_{0o} and Z_{0e} , using single microstrip line equation and free space characteristic impedance curve. In both case (w/h and s/h), there are two distinct stages. First stage, determination of equivalent single microstrip shape ratios $(w/h)_s$ for even and odd modes. The second stage, relates the required w/h and s/h for the coupled structure to the equivalent single microstrip shape ratios.

The final results are made independent of the substrate permittivity for a considerable range. The methodology of the design can be summarized as following;

- a) Determine shape ratios for equivalent single microstrip lines.
- b) Obtain the shape ratio w/h and spacing ratio s/h for the desired coupled microstrip structure using the single line shape ratios found at stage (a).

3.5.1 Microstrip Branch-Line Coupler Specification

- | | |
|---------------------|---------|
| 1. Center frequency | 2.0 GHz |
| 2. Coupling | 3.01 dB |
| 3. Insertion Loss | < -0.5 |
| 4. VSWR | < 2.0 |

Substrate ROGER RT/duroid® 5880 specification

Permittivity, ϵ_r = 2.20

Dielectric height, h = 0.79 mm

4.0 RESULT , MEASUREMENT & SIMULATION

4.1 Measurement of Filters

The measurement of the filters was done at the Radio Communication Laboratory UTM. Two different equipment was used for these measurements:

- i. Marconi Instruments.
 - MARCONI Test Set 6204 – 10 MHz to 26.5 GHz
 - Transmission line Test Head 6583 – 10 MHz – 26.5 GHz
 - 50 ohm Termination (dummy load) – Weischel
 - calibration short/open load
 - SMA connector cable (MA-COM) S/N: 2056-0000-00

This equipment is used to measure return loss, insertion loss and VSWR. Marconi analyzer is extremely useful and versatile instrument for the measurement of microwave signals in multiport networks. It is combination of a number of instruments in one package. This equipment integrated a synthesized sweep generator, a four input scalar analyzer, frequency counter and a power meter into one single compact case.

- ii. Signal Generator 2 GHz – 20 GHz. ROHDE & SCHWARZ
- iii Spectrum Analyzer – ADVAND TEST R4131D

This equipment is used to measure power (insertion loss) and operating frequency (pass band).

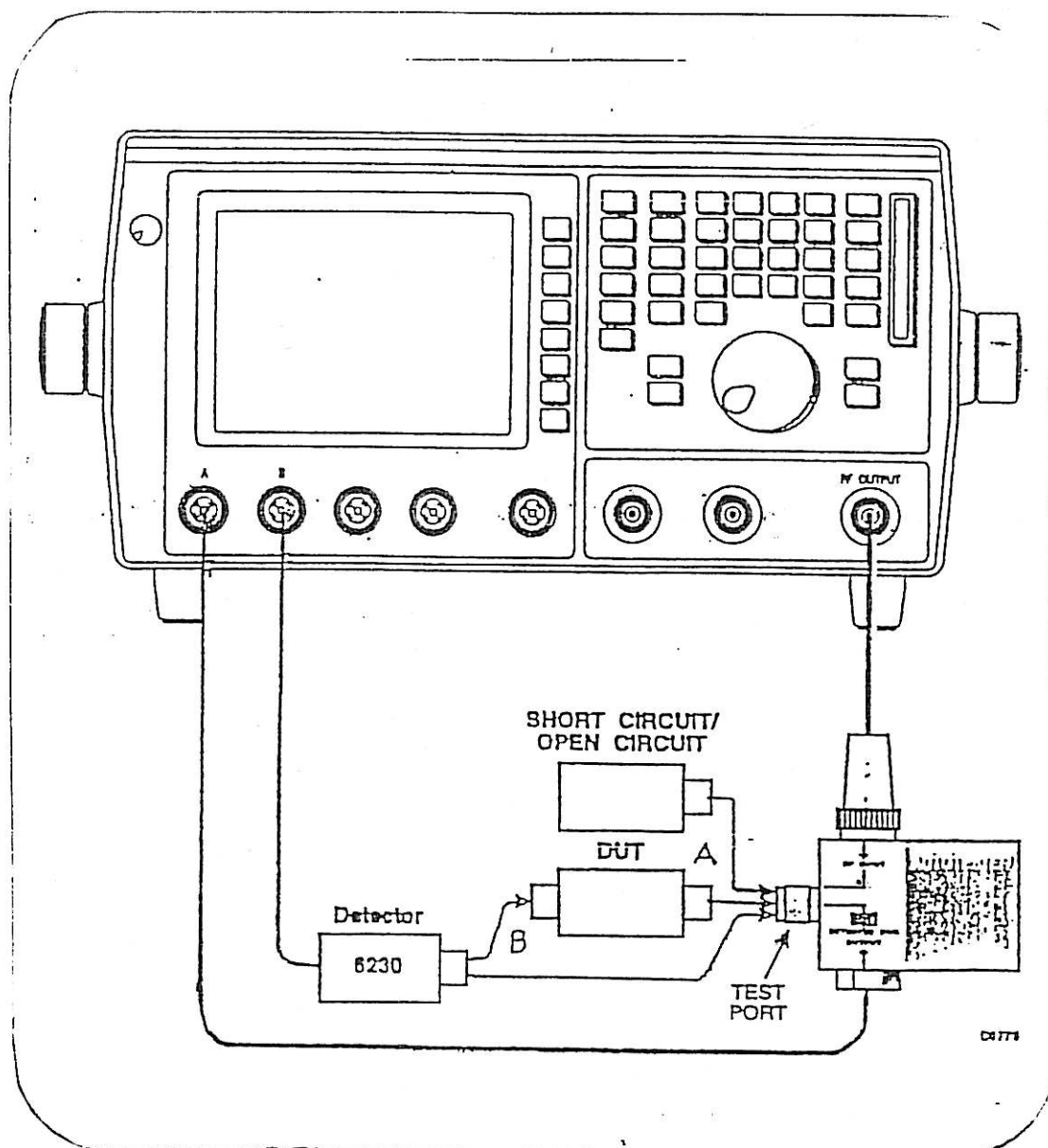


Figure 4.1 Set-up connection for the return loss, insertion loss and VSWR using Marconi equipment.

For the measurement of power and operating frequency, the Signal generator and Advantest Spectrum Analyzer is used. Following in the figure 4.2 is a block diagram of the measurement set-up connection.

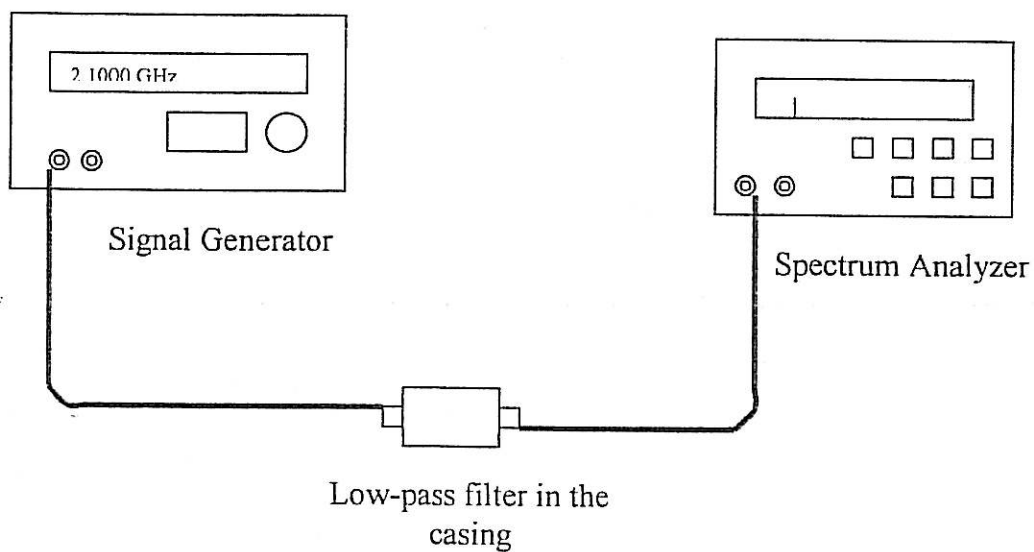


Figure 4.2 : Measurement system arrangement for measuring power (insertion loss) and operating frequency (pass band)

4.1.1 Filters Measurement Result

In this project, the result is based on actual measurement where scattering parameters S_{11} , S_{12} , S_{21} and S_{22} is being measured. The definition of each parameter are summarized as followed:

- S_{11} – input reflection coefficient with the output port terminated by a matched load.
- S_{12} – Reverse transmission (insertion) gain with the input port terminated in a matched load.

- S_{21} – Forward transmission (insertion) gain with the input port terminated in a matched load.
- S_{22} – Output reflection coefficient with the input terminated by a matched load.

On the other hand, S_{11} also defined as return loss and S_{21} is defined insertion loss. From both scattering parameter S_{21} is strongly influences the characteristic of the filter. In the actual measurement, the insertion loss (S_{21}) is measured by the scalar detector connector to input B and return loss (S_{11}) is measured by the autotester connected to input A. the results is plotted using a plotted and shown in Appendix H, I, J and K

4.1.2 Filters Simulation with PUFF

The design process is further continued with the utilisation of the .PUFF simulation. From the result of the simulation, the response of the band pass filter can be visualized. The design is analyzed according to the S-parameters which are displayed in the PUFF response. To obtain the results from the simulation the following steps should be followed:

- i. Key in the values for the even mode and the odd mode characteristics impedance in the parts window.
- ii. Do some adjustment of values in the broad window according to the type of substrate chosen.
 - a) The circuit of the band pass filter is drawn in the layout window.
 - b) Then from the plot window the response of the band pass filter can be obtained. The desired S-parameters should be notified in the

plot window. After reaching the plot window, the response can be plotted by typing 'p'.

- c) The dimension of the circuit are displayed by pressing '=' key in the parts window for each section of coupled lines.

In this design, only the value of S_{11} (return loss) and S_{21} (insertion loss) are taken into account. After the response is plotted, the values of S_{11} and S_{21} can be determined at the different point of frequencies. This can be done in the plot window by typing 'PgDn' and 'PgUp'.

The simulation process is started with the calculated values. Then, the simulations for the purpose of the optimization are done by doing some adjustment to the length of the resonators and increasing the order of the filters.

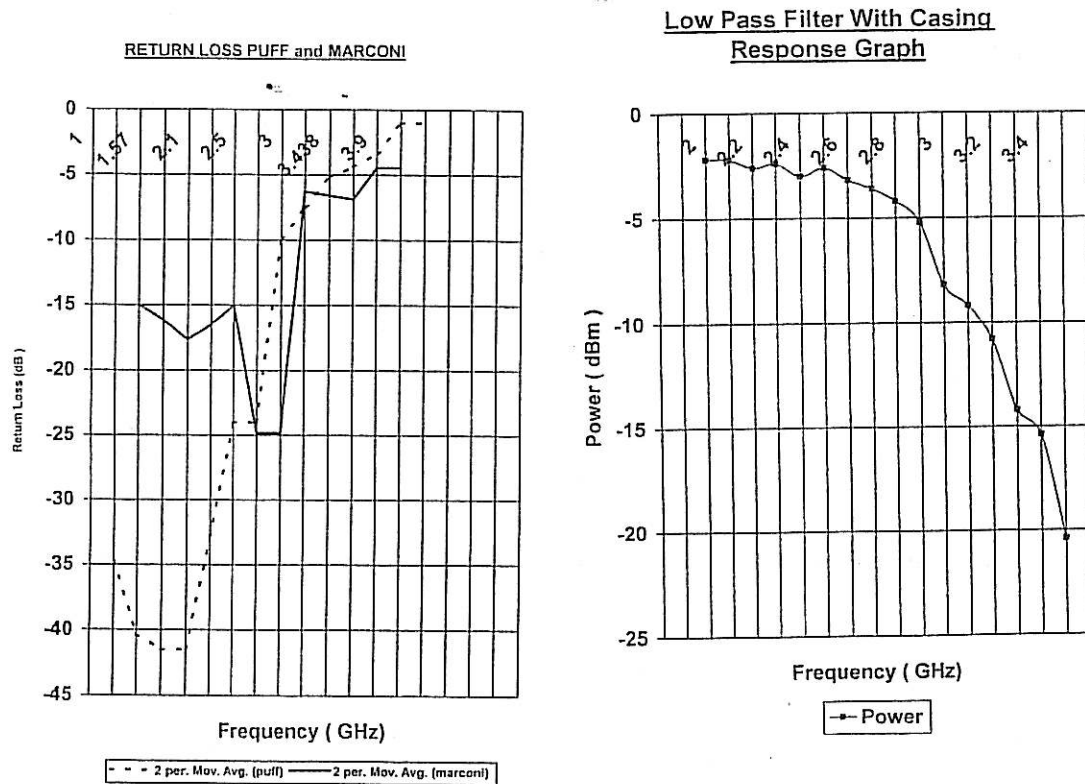


Figure 4.3: Low pass filter response simulation and measurement

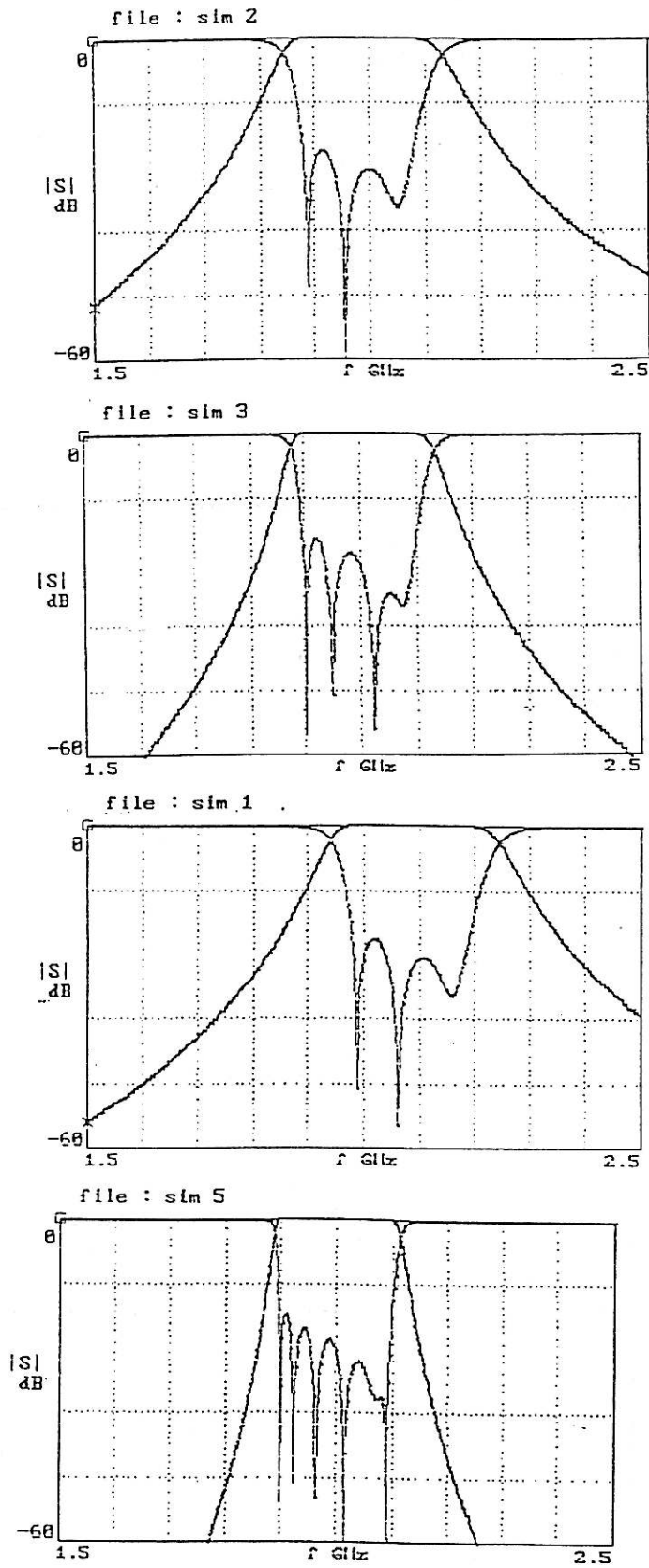
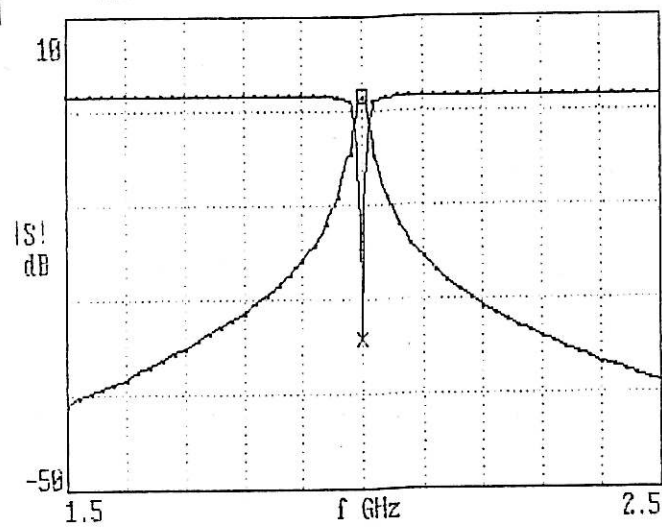
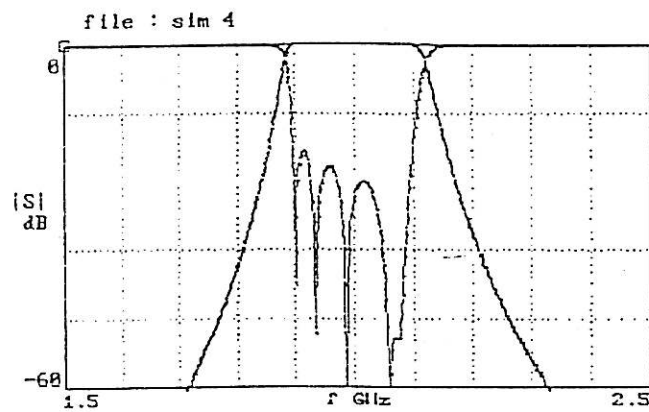


Figure 4.4 Band pass filter Response



(a) parallel line band stop filter



(b) open circuit stub band stop filter

Figure 4.5 Band Stop filter Response

4.2 Measurement of Microstrip Branch-Line Coupler

The measurement of the branch-line coupler was done at the Radio Communication Laboratory UTM. The same equipment is being used for measurement purpose. Two different equipments were used for these measurements :

i. Marconi Instruments

- Marconi Test Set 6204 – 10 MHz to 26.5 GHz
- Transmission line Test Head 6583 – 10 MHz to 26.5 GHz
- 50 Ω Termination (dummy load) – Weinschel
- calibration short /open load
- SMA connector cable

The equipment is being used to measure return loss and VSWR.

Marconi analyzer is extremely useful and versatile instrument for the measurement of microwave signals in multiport networks. It is combination of a number of instruments in one package. This equipment integrated a synthesized sweep generator, a four input scalar analyzer, frequency counter and a power meter into one single compact case. We can have the return loss measurement of the power divider when we connected the output of the Marconi Instrument to the return loss port at the Transmission Line Head. Meanwhile other ports are terminated with 50 Ω matching impedance.

ii Signal Generator 2 GHz – 20 GHz . SCROHDE & SCHWARZ

iii Spectrum Analyzer – ADVANTEST R4131D

The above equipment is used to measure power and operating frequency (pass band).

The coupling of return loss and insertion loss measurement of the branch-line coupler can be obtained by connecting the output of the Marconi Instrument to the return loss port at the Transmission Line Head. Meanwhile port 1, port 2 and port 4 are terminated with $50\ \Omega$ matching impedance. The measurement technique used for both return loss and insertion loss are same except for the changes in the channel A meanwhile for insertion loss channel B is being used.

4.2.1 Results of the Measurements

In this project, the result have been obtained from actual measurement where the scattering parameters S_{11} , S_{12} , S_{21} and S_{22} were measured. The result of measurement and simulation is shown as in figure 4.6- 4.11

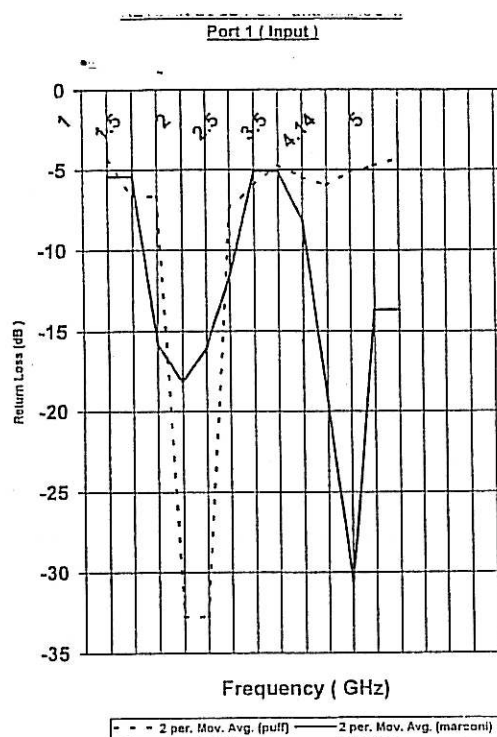


Figure 4.6 : Shows the comparison result between the return loss obtained from the simulation and the actual measurement using Marconi Instrument for port 1.

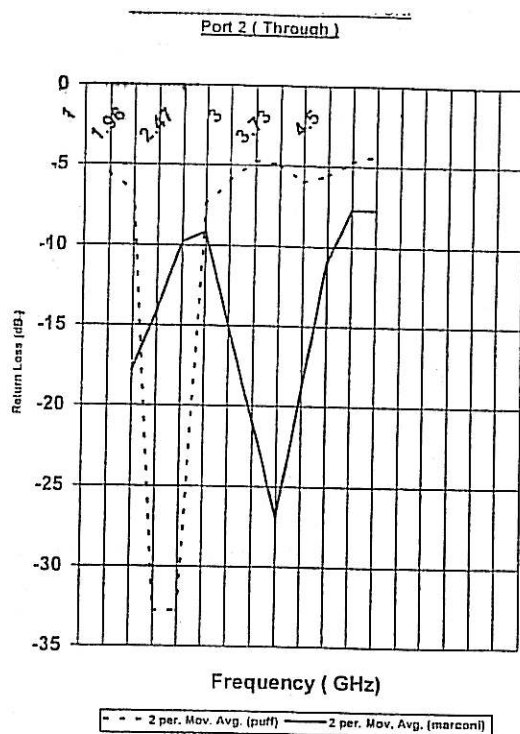


Figure 4.7 : Shows the comparison between the return loss obtained from the simulation and the actual measurement using Marconi Instrument for port 2

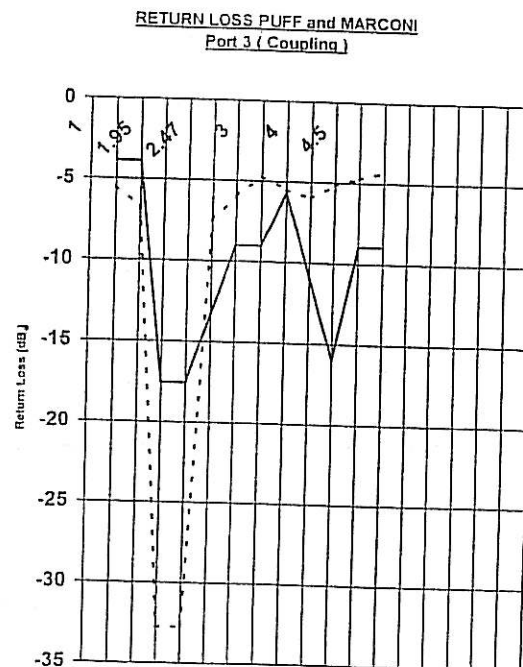


Figure 4.8 : Shows the comparison result between the return loss obtained from the simulation and the actual measurement using Marconi Instrument for port 3.

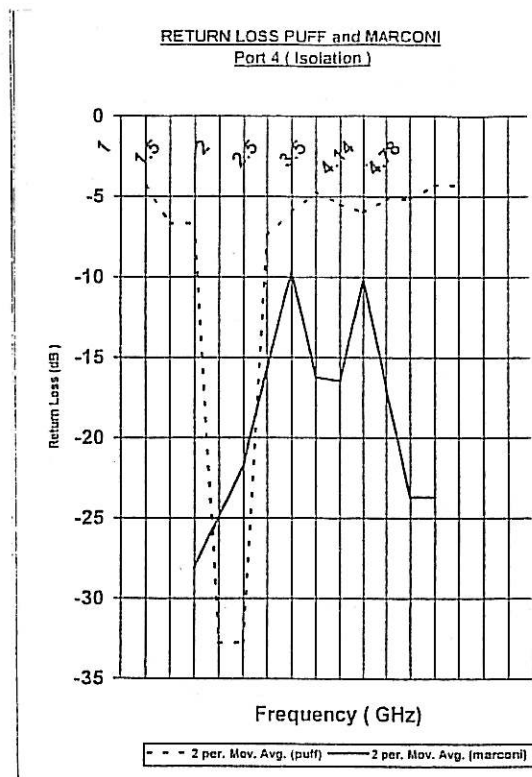


Figure 4.9 : Shows the comparison result between the return loss obtained from the simulation and the actual measurement using Marconi Instrument for port 4.

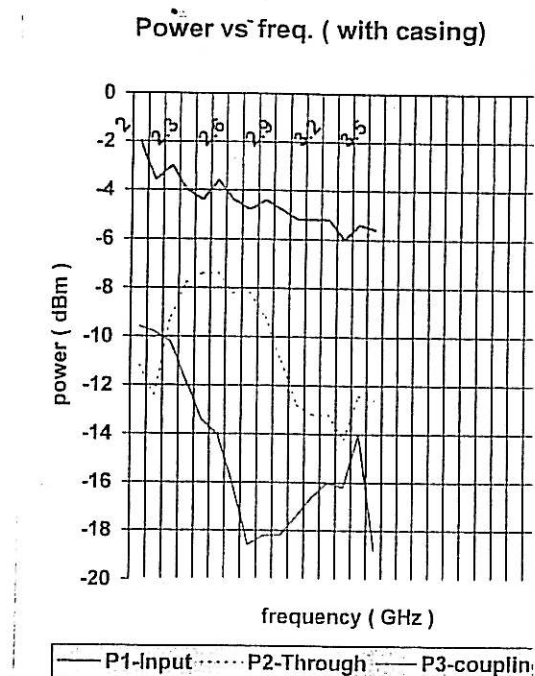


Figure 4.10 : Shows the power at port 1, port 2 and port 3 according to the reading obtain from the.

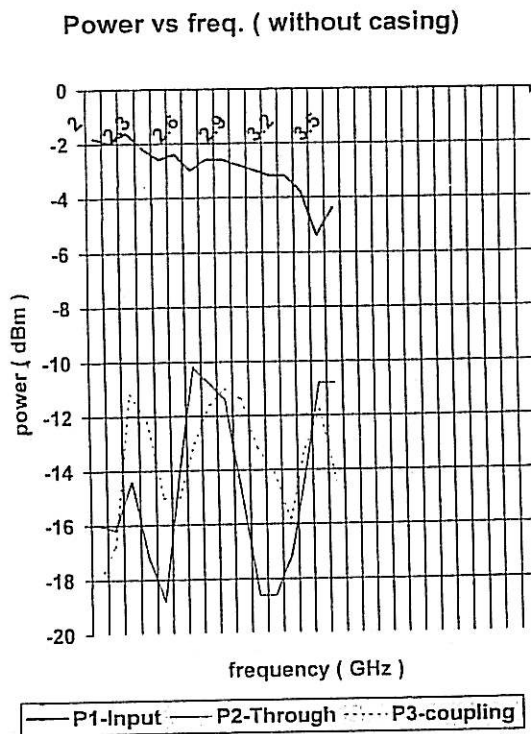


Figure 4.11 : Shows the power at port 1, port 2 and port 3 according to the reading obtain from table 4.2.5 (e)

4.3 Measurement and Analysis of Wilkinson Power Divider

4.3.1 Return loss measurement

Return loss referred to matching of the transmission line system which it forms a part, it causes reflection at the junctions between the line and the component. These reflections set up the standing wave pattern in the feed lines, as shown in figure 4.12. The type of instrument that is being used in laboratory for this testing purpose is the same equipment for filter measurement.

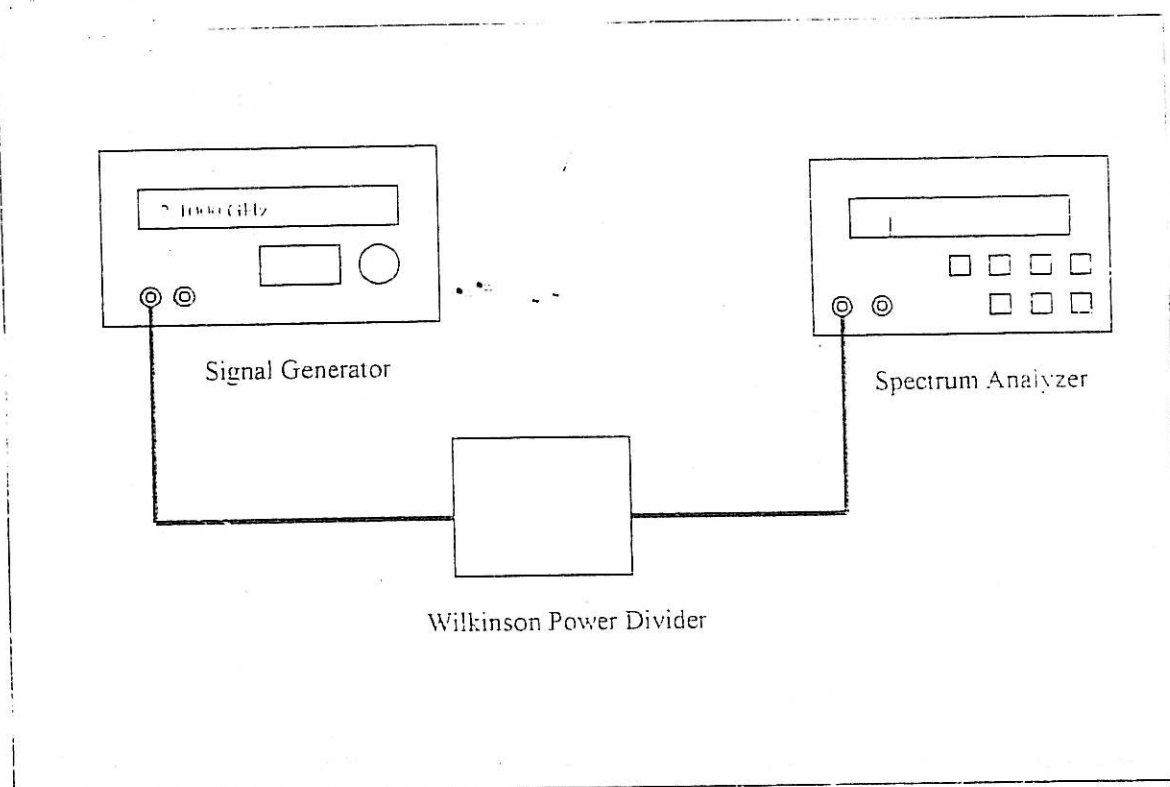


Figure 4.12 Set-up measurement for return loss, insertion loss and VSWR.

For the measurement of power and operating frequency, the Signal Generator and Advantest Spectrum analyzer is used. Figure 4.13 shows a block diagram of the measurement set up connection.

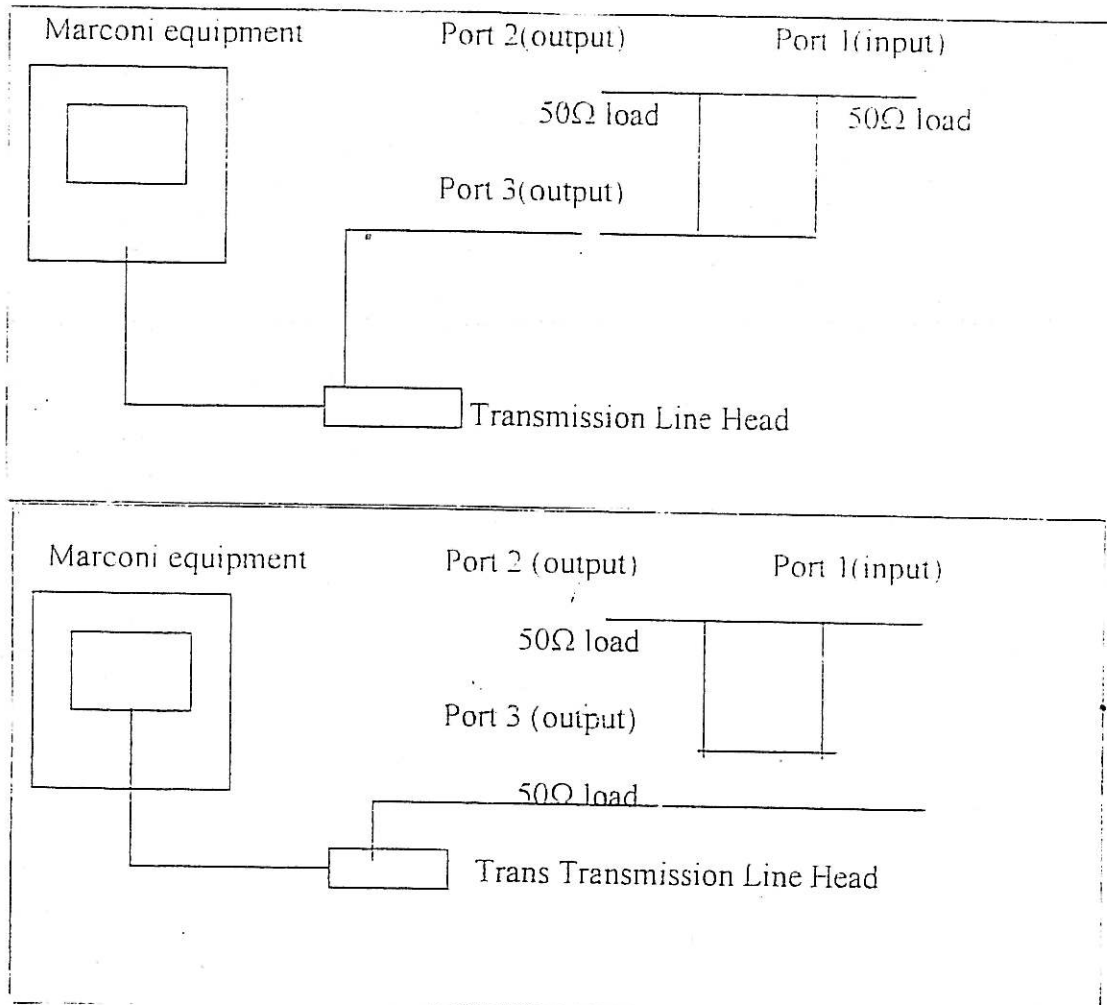


Figure 4.13 : Measurement system arrangement for measuring power and frequency operating.

4.3.2 Measurement Results for Wilkinson Power Divider

The results that obtained in this project are in terms of return loss or VSWR and power. The return loss for each ports are measured ; scattering parameters S_{11} , S_{22}

and S_{33} . Figure shows the result from measurement using Marconi instrument and spectrum analyzer and signal generator

4.3.3 Design Analysis

Basically, in this project there are two type of Wilkinson Power Divider which are uncompensated and compensated. Furthermore, in this project two shapes of power divider are discussed. It consists of mitered and radial bend shape. Analysis is being made for each shape. The comparison between simulation results and testing using instrument are made for uncompensated power divider in order to determine the bend shape with better efficiency (refer to figure 4.14). The comparison made in terms of return loss at each port.

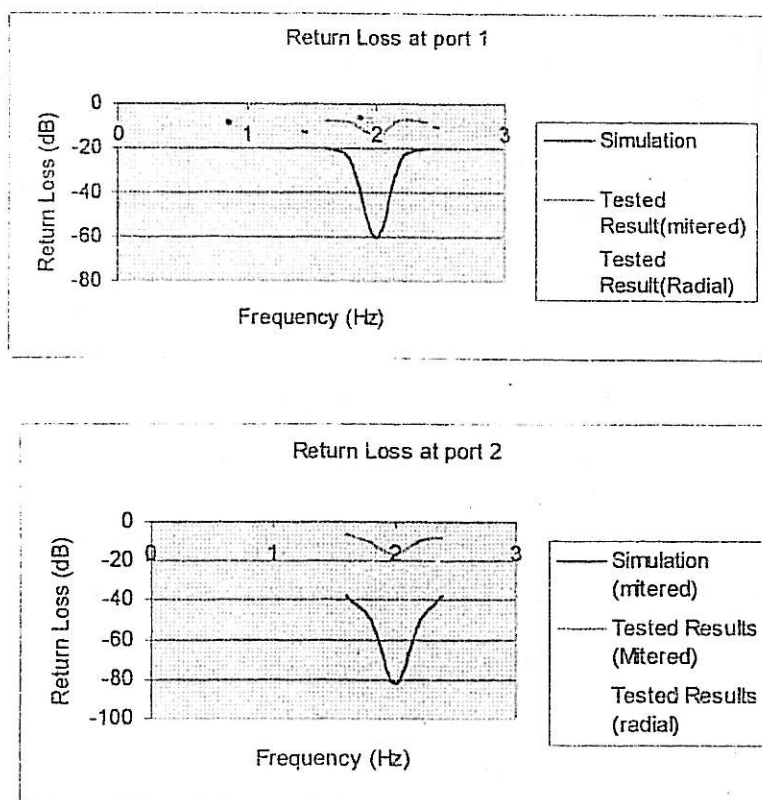


Figure 4.14 : Comparison between the simulation results and tested results for uncompensated Wilkinson Power Divider

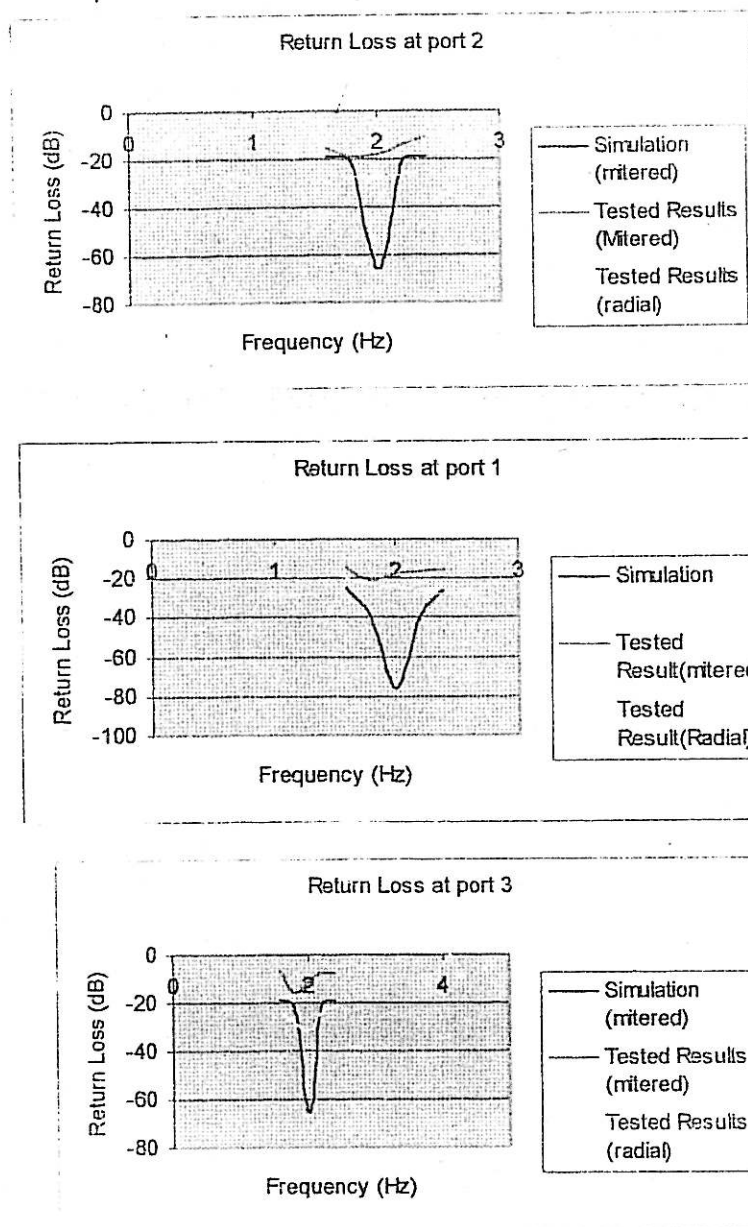


Figure 4.15 : Comparison between the simulation results and tested results for uncompensated Wilkinson Power Divider

5.0 DISCUSSION

5.1 FILTERS

At the design stage, all the parameters values are calculated manually to get the desired response. The filter circuits then was simulated by using the PUFF software package, where all the parameters values are key-in into this package for simulation and optimization purpose.

The design process of the filters is based on the S-parameters from the PUFF simulation. We are only concern about S_{11} (return loss) and S_{21} (insertion loss). The basic concept of the filter, the S_{11} value should be kept as low as possible, meanwhile the value of S_{21} should be kept at 0 dB. In order to achieve the best result, optimization was done. During the optimization process the analysis of the bandwidth and centre frequency were given more priority. It is realized that while doing optimization certain error parameters have to be sacrificed to maintain the minimum error in the bandwidth and the centre frequency.

In designing the microstrip low-pass filter, all the steps of calculation was done manually. So, it is really difficult to avoid errors during the works of designing and fabricating. What we can do is try to minimize these errors as low as possible. Humans, equipment and natural phenomenon are the factors can cause these unavoidable errors. The details of the errors could be occur are described below.

- Calculation – all the parameters in the design filter were calculated using typical calculator. Because of this, when dealing with small decimal numbers, some error maybe occurred.
- Assumption – some of the theoretical calculation is only based on some assumptions.

- Simulation – simulation using PUFF may have some errors because we don't know the actual formulas used in this software.
- Five order design gave a better response compared to a seven order design of the low pass filter using simulation of PUFF.

5.2 Branch Line Coupler

The branch-line coupler circuits was simulated by using the PUFF software package, where all the parameters values are key-in into this package for simulation and optimization purpose. From this simulation, the actual dimension is obtained. From the result obtained from the simulation the S_{11} gives the value of -40.56 dB at 2 GHz. It also has the insertion loss around -3.01 dB. Meanwhile from the measurement obtained from Marconi shows that for port 2, the best result of return loss is obtained at the center frequency of 3.72 that is -26.92 dB. The VSWR obtained at this frequency is 1.32. And the insertion loss is 0.31 dB.

For the port 3 (coupling) the best result of return loss is obtained at the cut off frequency of 2 GHz that's around -17.55 dB and VSWR is around 1.53 and the insertion loss is around 0.86 dB. Lastly for port 4 (isolation) the best result of return loss is obtained at the frequency of 1.98 GHz and the VSWR is 1.28 and it is having 1.27 dB insertion loss.

5.3 Wilkinson power Divider

The simulation results for compensated mitred bend shape power divider in terms of return loss are; $S_{11} = -60.6$ dB, $S_{22} = -82.5$ dB, $S_{33} = 82.5$ dB. And the value of scattering parameters for compensated mitred power divider ; $S_{11} = -76.3$ dB, S_{22}

= -65.9 dB, $S_{33} = -65.9$ dB. This results shows us that the output VSWR for compensated better than input VSWR, and the input VSWR for compensated better than output VSWR.

The tested results indicates that return loss for uncompensated mitered bend shape ; $S_{11} = -15.34$ dB, $S_{22} = -16.51$ dB, $S_{33} = -15.30$ dB. And for compensated mitered bend shape ; $S_{11} = -17.93$ dB, $S_{22} = -13.61$ dB, $S_{33} = -11.83$ dB. However, the radial bend shape value is more better than mitered bend shape. The return loss value for uncompensated radial bend shape; $S_{11} = -15.28$ dB, $S_{22} = -23.26$ dB, $S_{33} = -23.61$ dB. And the value for compensated radial bend shape ; $S_{11} = -24.37$ dB, $S_{22} = -17.48$ dB, $S_{33} = -21.47$ dB.

From the comparison above, the tested results of radial bend is better than mitered bend shape. Anyhow, the design still cannot achieve the simulation results due to fabrication process such as etching and soldering process. Practically, the mitered power divider are not a excellent design. Radial bend become choice of a microstrip's designer of the good performance. The quarter wave transformer must be brought closer because the negligible coupling need to avoid. In order to avoid the coupling, a good decision on discontinuity shape must be considered. As we the radial bend shape can provide less coupling effect compare to mitered shape.

Power division measurement indicates that at operating frequency for both uncompensated and compensated the equal division are occurred For each transmitting power varying from 0 dBm, 10 dBm and 20 dBm, the receiving power at output ports are divide equally. Even the power divide equally at output port but received power is very low where experienced losses in microstrip transmission line.

Losses as conductor loss, dielectric loss, radiation loss and surface wave loss are take place. This type of losses are categorized as microstrip transmission losses. External losses due to soldering also a major factor. The design furthered by doing in die cast box to minimize the microstrip losses. The loss is predicted to be minimum after been kept in die cast box.

The design furthered be fitted in die cast box. But the design did not show a good performance in casing as predicted. This is due to connector. The available is SMA connector which been used for design but it is not suitable for die cast box. This will lead to grounding problem as not achieved a good connection to ground. So, the project in casing is not successful and hopefully be continued by future student.

Basically, the value of VSWR for compensated is greater than uncompensated. This is due to compensated facing extra discontinuity effect (symmetrical step). This effect will lead to loss of microstrip transmission. The compensation made for reduce capacitance by shortened Δl at the length of quarter wave transformer to retain correct impedance at step. Anyhow, the perfect compensated design cannot be achieved as the etching tolerance occurred. So we cannot achieved the best compensation, hence excessive capacitance still appears. The explanation would be the possibility for the solution above.

After analyzing the design, the scattering parameters and power division are satisfied the design requirement.

6.0 CONCLUSION

From the overall results of simulation and analysis, it was notified that the stop band frequency for filter is depend on the resonators length. The width and separation are principally a function of characteristic impedance and thickness of the substrate. In designing the microstrip low pass filter all the steps of calculation was done manually. For the performance evaluation the comparison between the desired and the simulation response have difference where the cut off frequency at 3 dB shift from 2.1 GHz to 2.66 GHz. at 2.66 GHz the VSWR is 1.14 and return loss is -25.07 dB so it cut off aat 2.66 GHz. The shift of the cut off frequency of the low pass filter is due to the capacitance effect produced by in accurate etching process.

In designing the band pass filter the first optimisation is done by increasing the resonator length. In order to achieve the best result. During the optimisation process the anlaysisi of the bandwidth and center frequency were given more priority. It is realised that while doing optimistaion certain error of parametyers have to be sacrificed to maintain the minimum error in the bandwidth and the center frequency. From the overll result of simulation of bandpass filter it was notified that the operating frequency can be shifted by varying the resonators length. Furthernmore the result also [prove that the cut off response is sharper for the higher order filters

In designing bandstop filter, the result from calculation and comparison with PUFF is use to choose the best design. The design must be consider the value of return loss and insertion loss. For bandstop filter the coupling bandstop filter show a good performance compared with the stub bandstop filter. The value of the insertion loss for coupling bandstop filter design, is -31.06 dB. Compared to the value of

insertion loss for stub bandstop filter design, is -59.09 dB. That's mean, the performance for the coupling design is better than the stub bandstop filter design. The width and separation are principally a function of characteristic impedance and thickness of the substrate. For a chosen substrate these dimension values will not differ a lot, even though the operating frequency is varied. The physical length of the resonators simply depend on the wavelength.

How ever, in practically the performance for coupling bandstop design compared with stub bandstop design, is not same as the result we get from the simulation with PUFF. Analysis for fabrication bandstop filter (stub) is better than the coupling bandstop filter. From the measurement, the matching of return loss and VSWR for bandstop filter by using the stub design have a good matching at lower frequency (1.17 GHz) and upper frequency (3.34 GHz) with the value of VSWR is 1.10 and 1.16 . Compared to the coupling bandstop design at lower frequency (1.90 GHz) and upper frequency (3.74 GHz) with the value of VSWR is 1.23 1.57 .

As a conclusion, practically the bandstop filter design using stub performance is better than the bandstop filter design using coupling, although in theoretical and simulation from PUFF is show the coupling bandstop filter is better. This is because in practically, to fabricate the coupling bandstop filter is quite hard compared with stub bandstop filter. The space between each coupling give an effect to performance of the filter consider to the losses and the electromagnetic field.

The design stage for branch line coupler are calculated manually to get the desired response. The design and fabrication of microstrip branch line coupler provides a guide line to produce the hardware according to the given specification. Maximum coupling occurs at $\lambda/4$ which means at this length the maximum signal is

coupled at the center frequency 2 GHz and this coupling happens at even and odd mode of the microwave propagation. Therefore even and odd mode analysis was implemented in the design methodology

For Wilkinson power divider design it is depend on the shape of the bending that used in quarter wave transformer. Selecting the good bending shape such as radial bend shape will perform a better result. In this project, it is obvious that the performance of the radial bend shape is better and efficient compared to the mitered bend shape. The testing of the casing and without casing made. However, the testing of. uncompensated and compensated without casing has been successful. Unfortunately, for the casing it is facing problems. The problems are due to grounding connection problem where the connector that provided not suitable for die cast box.

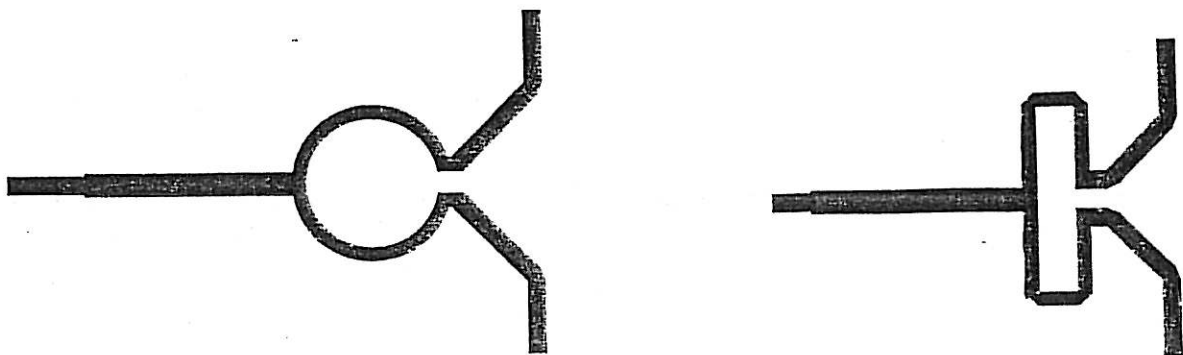
REFERENCE

- [1] Terry Edwards., 'Foundations for microstrip design', 2nd edition, John Wiley and sons 1995
- [2] Akhtarzad, S., Rowbotham, T.R., Jones, P.B., ' The design of coupled microstrip lines', IEEE Trans MTT-23 No 6 June 1975
- [3] E. H. Fooks, R. A. Zakrevicous, 'Microwave Engineering Using Microstrip Circuits, Prentice Hall, 1990
- [4] Dydyk,M., 'Accurate design of microstrip directional couplers with capacitive compensation', IEEE MTT-S International Microwave Symposium 1990.
- [5] Kajfez,D.,and Govind, S., 'Effects of difference in odd and even mode wavelength on a parallel coupled bandpass filter' , Electron.Lett., March 1975.
- [6] Matthaei, G.L., Young ,L.,and Jones, E.M.T., Microwave Filters, Impedance – Matching Networks and Coupling Structures, Mc Graw Hill ,New York 1965
- [7] Chris Bowick , 'RF Circuit Design', Indiana polis, Indiaana, Howard Sam & Con Inc 1982
- [8] Getsinger, W.J. , 'Dispersion of parallel Coupled Microstrip' , IEEE trans MTT- 21 1973
- [9] Edward A. Wolf, Roger Kaul, 'Microwave Engineering and Systems Application' , John Wiley & Sons 1988

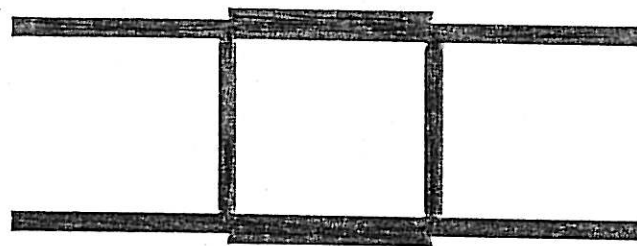
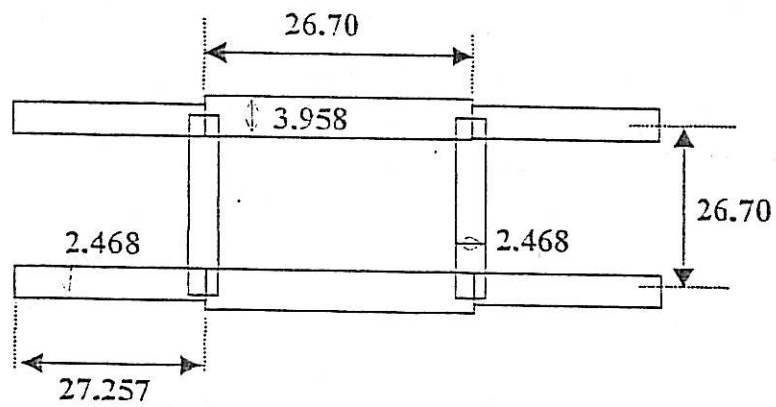
APPENDIX



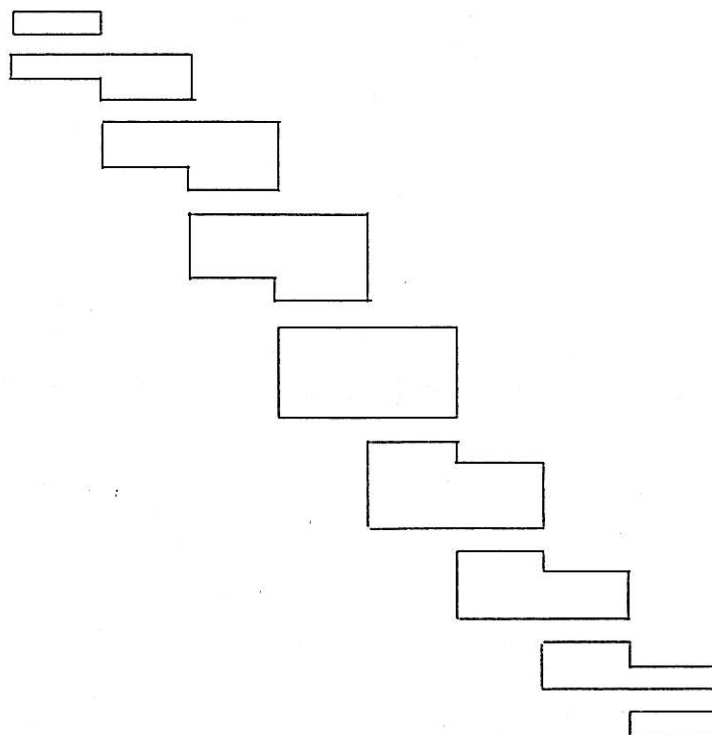
Microstrip uncompensated Wilkinson Power Divider layout



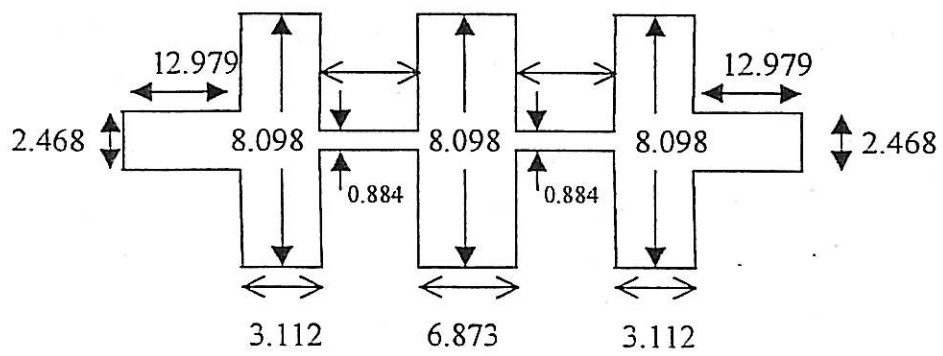
Microstrip compensated Wilkinson Power Divider Layout



Microstrip Hybrid Braanch Line Coupler Layout



Parallel Bandpass Filter Microstrip layout

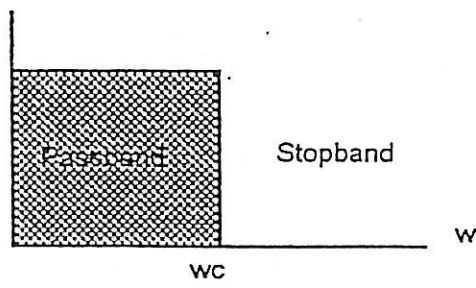


Microstrip Low pass Filter layout

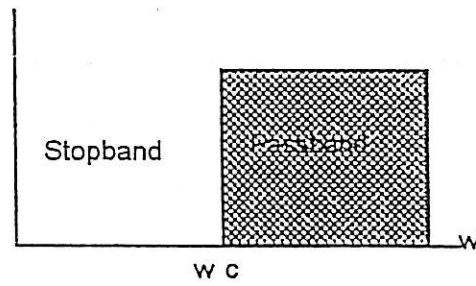
Material	ϵ_r	$\tan\delta$ @ 10 GHz	Advantages	Disadvantages
Air	1.0006	≈ 0	Pure TEM wave. Assumed as free space	No support for strip. Large physically size. High thermal expansion. Poor mechanical properties.
PTFE	2.1	0.0003		High thermal expansion. Variability between batches.
Reinforced plastics	2.3 - 2.6	< 0.0001	Improved mechanical properties.	High thermal expansion. Variability between batches.
Quartz	3.78	0.0001	Reproducible substrate. Useful in mm range. Low thermal expansion. Good mechanical properties.	Variability between batches.
Ceramic loaded plastics.	2.5 - 10	< 0.002		
Alumina 99.5% pure	9.8	0.0001	Reproducible substrate-improving with purity.	Brittle. Slightly anisotropic.
Sapphire	9.4	0.0001	Reproducible substrates. Very smooth surfaces.	Anisotropic crystal. Small size-high cost.
Al_2O_3	11.6		Integration with high frequency active devices.	Thin substrates (~0.15mm)
GaAs	12.9	0.002	Reduced size component	Rough surfaces.
Rutile TiO_2	85	0.004		Temperature sensitive ϵ_r .

The properties of substrate materials

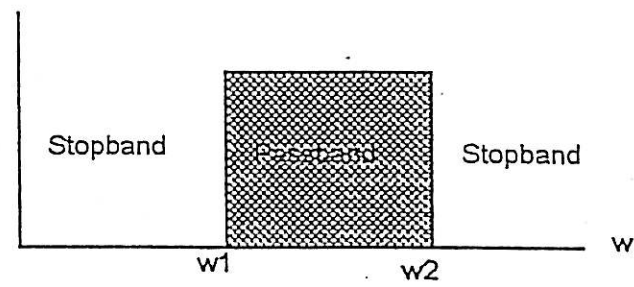
Ideal Filter Design



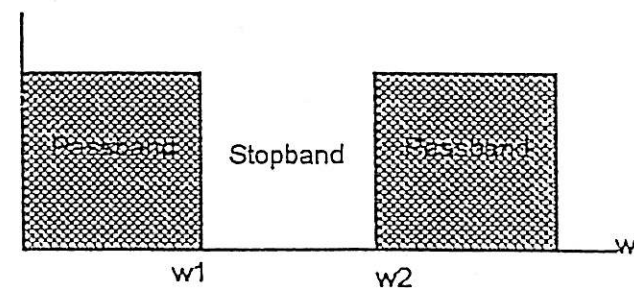
a) Lowpass filter



b) Highpass



c) Bandpass



d) Bandstop

The ideal "brick-wall" response of four types of filter

Dissipating constant, C	1MHz, MIL-P-13949G Appendix U	C 24/23/50	Z	2.20	
	10GHz, IPC-TM-650, 2.5.5.5	C 24/23/50	Z	2.20 ± 0.02 spec.	
	1MHz, MIL-P-13949G Appendix B	C 24/23/50	Z	0.0004	
	10GHz, IPC-TM-650, 2.5.5.5	C 24/23/50	Z	0.0009	
Volume resistivity	ASTM D257	C96/35/90	Mohm cm	Z	2 x 10 ⁷
Surface resistivity	ASTM D257	C96/35/90	Mohm	X,Y	3 x 10 ⁵
Tensile modulus	ASTM D638	A	MPa (kpsi)	X	1070 (156)
ultimate stress				Y	450 (65)
ultimate strain			MPa (kpsi)	X	860 (125)
				Y	300 (55)
Compressive modulus			%	X	29 (4.2)
				Y	20 (2.9)
ultimate stress				X	27 (3.9)
				Y	18 (2.6)
ultimate strain			MPa (kpsi)	X	6.9
				Y	7.2
Deformation under load			MPa (kpsi)	X	4.9
				Y	5.8
Water absorption			MPa (kpsi)	X	710 (103)
				Y	500 (73)
Specific gravity			MPa (kpsi)	Z	710 (103)
				X	500 (75)
Thermal expansion			%	Y	670 (97)
				Z	27 (3.9)
Thermal conductivity				X	22 (3.2)
				Y	21 (3.1)
Thermal distortion temperature				Z	21 (3.1)
				X	52 (7.5)
Thermal heat				Y	43 (6.3)
				Z	0.4
Thermal modulus				X	7.7
				Y	12.5
Thermal expansion				Z	17.6
				X	0.9 (0.02)
Thermal conductivity				Y	1.3 (0.015)
				Z	2.2
Thermal distortion temperature				X,Y	>260 (>500)
				Z	0.96 (0.23)
Thermal heat				X	0.26 (1.8)
				Y	Z
Thermal modulus				X	-6.1
				Y	-18.7
Thermal expansion				Z	-1.8
				X	-0.9
Thermal distortion temperature				Y	-0.5
				Z	-4.5
Thermal heat				X	1.1
				Y	1.5
Thermal modulus				Z	8.7
				X	2.3
Thermal expansion				Y	3.8
				Z	5.5
Thermal distortion temperature				X	2.3
				Y	3.8
Thermal heat				Z	5.5
				X	2.3
Thermal modulus				Y	3.8
				Z	5.5
Thermal expansion				X	2.3
				Y	3.8
Thermal distortion temperature				Z	5.5
				X	2.3
Thermal heat				Y	3.8
				Z	5.5
Thermal modulus				X	2.3
				Y	3.8
Thermal expansion				Z	5.5
				X	2.3
Thermal distortion temperature				Y	3.8
				Z	5.5
Thermal heat				X	2.3
				Y	3.8
Thermal modulus				Z	5.5
				X	2.3
Thermal expansion				Y	3.8
				Z	5.5
Thermal distortion temperature				X	2.3
				Y	3.8
Thermal heat				Z	5.5
				X	2.3
Thermal modulus				Y	3.8
				Z	5.5
Thermal expansion				X	2.3
				Y	3.8
Thermal distortion temperature				Z	5.5
				X	2.3
Thermal heat				Y	3.8
				Z	5.5
Thermal modulus				X	2.3
				Y	3.8
Thermal expansion				Z	5.5
				X	2.3
Thermal distortion temperature				Y	3.8
				Z	5.5
Thermal heat				X	2.3
				Y	3.8
Thermal modulus				Z	5.5
				X	2.3
Thermal expansion				Y	3.8
				Z	5.5
Thermal distortion temperature				X	2.3
				Y	3.8
Thermal heat				Z	5.5
				X	2.3
Thermal modulus				Y	3.8
				Z	5.5
Thermal expansion				X	2.3
				Y	3.8
Thermal distortion temperature				Z	5.5
				X	2.3
Thermal heat				Y	3.8
				Z	5.5
Thermal modulus				X	2.3
				Y	3.8
Thermal expansion				Z	5.5
				X	2.3
Thermal distortion temperature				Y	3.8
				Z	5.5
Thermal heat				X	2.3
				Y	3.8
Thermal modulus				Z	5.5
				X	2.3
Thermal expansion				Y	3.8
				Z	5.5
Thermal distortion temperature				X	2.3
				Y	3.8
Thermal heat				Z	5.5
				X	2.3
Thermal modulus				Y	3.8
				Z	5.5
Thermal expansion				X	2.3
				Y	3.8
Thermal distortion temperature				Z	5.5
				X	2.3
Thermal heat				Y	3.8
				Z	5.5
Thermal modulus				X	2.3
				Y	3.8
Thermal expansion				Z	5.5
				X	2.3
Thermal distortion temperature				Y	3.8
				Z	5.5
Thermal heat				X	2.3
				Y	3.8
Thermal modulus				Z	5.5
				X	2.3
Thermal expansion				Y	3.8
				Z	5.5
Thermal distortion temperature				X	2.3
				Y	3.8
Thermal heat				Z	5.5
				X	2.3
Thermal modulus				Y	3.8
				Z	5.5
Thermal expansion				X	2.3
				Y	3.8
Thermal distortion temperature				Z	5.5
				X	2.3
Thermal heat				Y	3.8
				Z	5.5
Thermal modulus				X	2.3
				Y	3.8
Thermal expansion				Z	5.5
				X	2.3
Thermal distortion temperature				Y	3.8
				Z	5.5
Thermal heat				X	2.3
				Y	3.8
Thermal modulus				Z	5.5
				X	2.3
Thermal expansion				Y	3.8
				Z	5.5
Thermal distortion temperature				X	2.3
				Y	3.8
Thermal heat				Z	5.5
				X	2.3
Thermal modulus				Y	3.8
				Z	5.5
Thermal expansion				X	2.3
				Y	3.8
Thermal distortion temperature				Z	5.5
				X	2.3
Thermal heat				Y	3.8
				Z	5.5
Thermal modulus				X	2.3
				Y	3.8
Thermal expansion				Z	5.5
				X	2.3
Thermal distortion temperature				Y	3.8
				Z	5.5
Thermal heat				X	2.3
				Y	3.8
Thermal modulus				Z	5.5
				X	2.3
Thermal expansion				Y	3.8
				Z	5.5
Thermal distortion temperature				X	2.3
				Y	3.8
Thermal heat				Z	5.5
				X	2.3
Thermal modulus				Y	3.8
				Z	5.5
Thermal expansion				X	2.3
				Y	3.8
Thermal distortion temperature				Z	5.5
				X	2.3
Thermal heat				Y	3.8
				Z	5.5
Thermal modulus				X	2.3
				Y	3.8
Thermal expansion				Z	5.5
				X	2.3
Thermal distortion temperature				Y	3.8
				Z	5.5
Thermal heat				X	2.3
				Y	3.8
Thermal modulus				Z	5.5
				X	2.3
Thermal expansion				Y	3.8
				Z	5.5
Thermal distortion temperature				X	2.3
				Y	3.8
Thermal heat				Z	5.5
				X	2.3
Thermal modulus				Y	3.8
				Z	5.5
Thermal expansion				X	2.3
				Y	3.8
Thermal distortion temperature				Z	5.5
				X	2.3
Thermal heat				Y	3.8
				Z	5.5
Thermal modulus				X	2.3
				Y	3.8
Thermal expansion				Z	5.5
				X	2.3
Thermal distortion temperature				Y	3.8
				Z	5.5
Thermal heat				X	2.3
				Y	3.8
Thermal modulus				Z	5.5
				X	2.3
Thermal expansion				Y	3.8
				Z	5.5
Thermal distortion temperature				X	2.3
				Y	3.8
Thermal heat				Z	5.5
				X	2.3
Thermal modulus				Y	3.8
				Z	5.5
Thermal expansion				X	2.3
				Y	3.8
Thermal distortion temperature				Z	5.5
				X	2.3
Thermal heat				Y	3.8
				Z	5.5
Thermal modulus				X	2.3
				Y	3.8
Thermal expansion				Z	5.5
				X	2.3
Thermal distortion temperature				Y	3.8
				Z	5.5
Thermal heat				X	2.3
				Y	3.8
Thermal modulus				Z	5.5
				X	2.3
Thermal expansion				Y	3.8
				Z	5.5
Thermal distortion temperature				X	2.3
				Y	3.8
Thermal heat				Z	5.5
				X	2.3
Thermal modulus				Y	3.8
				Z	5.5
Thermal expansion				X	2.3
				Y	3.8
Thermal distortion temperature				Z	5.5
				X	2.3
Thermal heat				Y	3.8
				Z	5.5
Thermal modulus				X	2.3
				Y	3.8
Thermal expansion				Z	5.5
				X	2.3
Thermal distortion temperature				Y	3.8
				Z	5.5
Thermal heat				X	2.3
				Y	3.8
Thermal modulus				Z	5.5
				X	2.3
Thermal expansion				Y	3.8
				Z	5.5
Thermal distortion temperature				X	2.3
				Y	3.8
Thermal heat				Z	5.5
				X	2.3
Thermal modulus				Y	3.8
				Z	5.5
Thermal expansion				X	2.3
				Y	3.8
Thermal distortion temperature				Z	5.5
				X	2.3
Thermal heat				Y	3.8
				Z	5.5
Thermal modulus				X	2.3
				Y	3.8
Thermal expansion				Z	5.5
				X	2.3
Thermal distortion temperature				Y	3.8
				Z	5.5
Thermal heat				X	2.3
				Y	3.8
Thermal modulus				Z	5.5
				X	2.3
Thermal expansion				Y	3.8
				Z	5.5
Thermal distortion temperature				X	2.3
				Y	3.8
Thermal heat				Z	5.5
				X	2.3
Thermal modulus				Y	3.8
				Z	5.5
Thermal expansion				X	2.3
				Y	3.8
Thermal distortion temperature				Z	5.5
				X	2.3
Thermal heat				Y	3.8
				Z	5.5
Thermal modulus				X	2.3
				Y	3.8
Thermal expansion				Z	5.5
				X	2.3
Thermal distortion temperature				Y	3.8
				Z	5.5
Thermal heat				X	2.3
				Y	3.8
Thermal modulus				Z	5.5
				X	2.3
Thermal expansion				Y	3.8
				Z	5.5
Thermal distortion temperature				X	2.3
				Y	3.8
Thermal heat				Z	5.5
				X	2.3
Thermal modulus					

RT/duroid® 5880

Glass Microfiber Reinforced

Polytetrafluoroethylene Composite

RT/duroid® 5880 glass microfiber reinforced PTFE composite is designed for exacting stripline and microstrip circuit applications.

Glass reinforcing microfibers are randomly oriented to maximize benefits of fiber reinforcement in the directions most valuable to circuit producers and in the final circuit application.

The dielectric constant of RT/duroid 5880 laminates is uniform from panel to panel and is constant over a wide frequency range. Its low dissipation factor extends the usefulness of 5880 to Ku-band and above.

RT/duroid 5880 laminate is easily cut, sheared and machined to shape. It has excellent dimensional stability and is resistant to all solvents and reagents, hot or cold, normally used in etching printed circuits or in plating edges and holes.

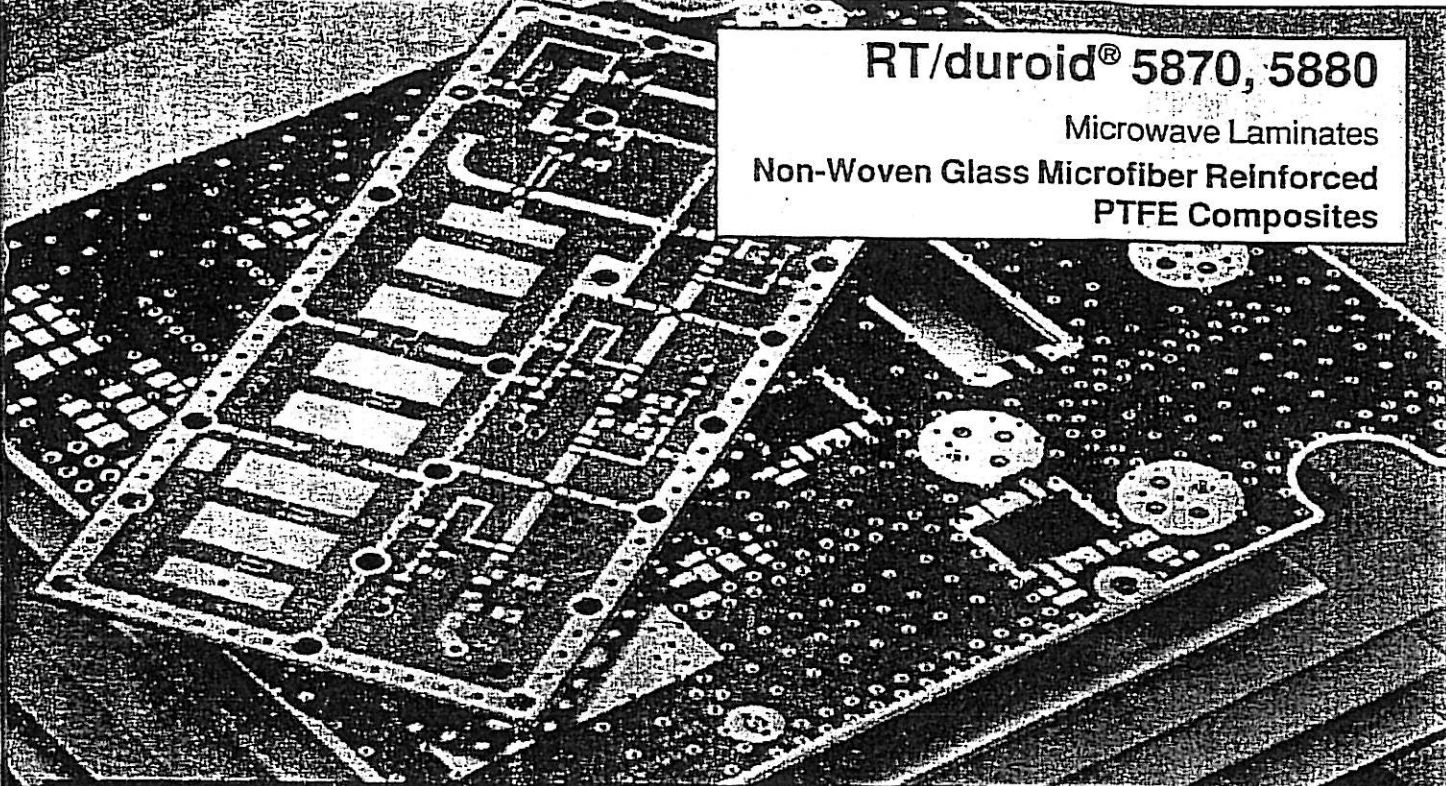
Normally supplied as a laminate with electro-deposited copper of 1/4 to 2 ounces/ft² on both sides. RT/duroid 5880 composites can also be clad with rolled copper foil for more critical electrical applications. Cladding with aluminum, copper or brass plate may also be specified.

When requested copper-clad, RT/duroid 5880 composite can be certified to MIL-P-13949 Type GRN or Type GPN microwave material specifications.

When ordering RT/duroid 5880 laminates, it is important to specify dielectric thickness, tolerance, rolled or electrodeposited copper foil, and weight of copper foil required.

(See reverse for product data)





RT/duroid® 5870, 5880

Microwave Laminates
Non-Woven Glass Microfiber Reinforced
PTFE Composites

Features and Benefits:

Meets Mil-S-13949.

- Suitable for military applications.

Lowest electrical loss for reinforced PTFE material.

- Provides low insertion loss.
- Able to design high Q circuits.

Low moisture absorption.

- No special storage requirements.
- Reduces effects of moisture on electrical loss.

Isotropic.

- Improved performance on filters and directional couplers.

Uniform electrical properties over frequency.

- Repeatable designs.
- Suitable for very broadband applications.

Excellent chemical resistance.

- Immune to effects of typical processing chemicals.

Typical Applications:

*Commercial Airline Telephones
Microstrip and Stripline Circuits
Millimeter Wave Applications
Military Radar Systems
Missile Guidance Systems
Point to Point Digital Radios*

Optimum Frequency Range:
1-90 GHz



ROGERS

Property/Units		Typical Values	
		RT/duroid 5880	RT/duroid 5870
Dielectric Constant @ 10 GHz		2.20 ± 0.02	2.33 ± 0.02
Thermal Coefficient of ϵ_r @ 0 to 100°C	ppm/°C	-129	-115
Dissipation Factor @ 10 GHz		0.0009	0.0012
Tensile Modulus X	kpsi	156	189
Y		125	185
Volume Resistivity	Mohm•cm	2 X 10 ⁷	2 X 10 ⁷
Surface Resistivity	Mohm	3 X 10 ⁸	2 X 10 ⁸
Compressive Modulus Z axis	kpsi	136	120
Moisture Absorption	%	0.015	0.015
Thermal Conductivity	W/m/K	0.20	0.22
Coefficient of Thermal Expansion 0 to 100°C X	ppm/°C	31	22
		48	28
		237	173
Specific Gravity		2.2	2.2

Rogers laminates can be purchased by contacting your U.S. customer service representative or one of our overseas offices. Telephone numbers listed below.

DUROID and DUROID are trademarks of Rogers Corporation for their microwave laminates.

Above data represents typical values, not statistical minimums. It is not intended to and does not create any warranties, express or implied, including any warranty of merchantability or fitness for a particular use. The relative merits of materials for a specific application should be determined by your evaluation.

ROGERS

Rogers Corporation
Microwave Materials Division
100 S. Roosevelt Avenue
Mesa, AZ 85226-3415
Tel: 602-961-1382 FAX: 602-961-4533
Website: <http://www.rogers-corp.com>
ISO 9002 CERTIFIED

In Japan:
Rogers Japan Inc.
7th Floor, ST Bldg.
2-26-9 Nishi-nippori
Arakawa-ku
Tokyo 116 Japan
03 3807 6430
FAX: 03 3807 6319

In Hong Kong:
Rogers Southeast Asia
21st Floor, Unit 2
118 Connaught Road West
Sheung Wan, Hong Kong
852-2549-7806
FAX: 852-2549-8615

In Europe:
Rogers N.V.
Afrikalaan 188
B-9000
Gent, Belgium
32-9-2353611
FAX: 32-9-2353658

Rogers High Frequency Circuit Material

Property		RT/duroid® 5880 (GR/GP)	RT/duroid® 5870 (GR/GP)	ULTRALAM® 2000 (GX)	RT/duroid® 6002	RT/duroid® 6006	RT/duroid® 6010LM	TMM® 3	TMM® 4	TMM® 6	TMM® 10	TMM® 10i
Composition		PTFE Glass Fiber	PTFE Glass Fiber	PTFE Woven Glass	PTFE Ceramic	PTFE Ceramic	PTFE Ceramic	Hydro- Carbon Ceramic	Hydro- Carbon Ceramic	Hydro- Carbon Ceramic	Hydro- Carbon Ceramic	Hydro- Carbon Ceramic
$\epsilon_r^{(1)}$ Tolerance		2.20 ±0.020	2.33 ±0.020	2.40-2.60 ±0.040	2.94 ±0.040	6.15 ±0.150	10.2 ±0.250	3.27 ±0.016	4.50 ±0.045	6.00 ±0.080	9.20 ±0.250	9.80 ±0.245
Tan δ		0.0009	0.0012	0.0019	0.0012	0.0019	0.0023	0.0020	0.0020	0.0023	0.0023	0.0020
Thermal coeff. of $\epsilon_r^{(2)}$ -50° to 150°C ppm/°C (Typical)		-125	-115	-100	+12	-410	-425	+39	—	+10	+38	+43
Volume resistivity Mohm-cm (Typical)		2x10 ¹²	2x10 ¹²	2x10 ¹²	10 ¹²	2x10 ¹²	5x10 ¹²	3x10 ¹²	6x10 ¹²	1x10 ¹³	2x10 ¹²	—
Surface resistivity Mohm (Typical)		3x10 ¹²	2x10 ¹²	4x10 ¹²	10 ¹²	7x10 ¹²	5x10 ¹²	>9x10 ¹²	1x10 ¹³	1x10 ¹³	4x10 ¹²	—
Young's Modulus ⁽³⁾	X - kpsi (MPa)	156 (1076)	189 (1340)	1700 (11,730)	120 (828)	74 (511)	135 (932)	1916 (13,210)	2000* (13,790)	2200 (15,168)	2400 (16,547)	—
	Y - kpsi (MPa)	125 (863)	185 (1277)	1300 (8970)	120 (828)	91 (628)	81 (559)	1916 (13,210)	2000* (13,790)	2200* (15,168)	2400 (16,547)	—
	Z - kpsi (MPa)	136 (938)	120 (828)	—	360* (2482)	155 (1070)	311 (2146)	742 (5116)	752 (5185)	736 (5075)	575 (3964)	—
Moisture ⁽⁴⁾ absorption D24/23% (Typical)		0.015	0.015	0.03	0.1	0.05	0.05	+0.04	+0.010	+0.06	+0.09	+0.16
Thermal ⁽⁵⁾ conductivity W/m·°K (Typical)		0.20	0.22	0.24	0.60	0.49	0.78	0.70	0.70	0.72	0.76	0.76
Coefficient of Thermal Expansion ppm/°C ⁽⁶⁾ 0° to 100°C (typ)	X	31	22	15	16	47	24	16	14	16	16	16*
	Y	48	28	15	16	34	24	16	14	16	16	16*
	Z	237	173	200	24	117	24	20	20	20	20	20*
Density gm/cm ³ (typical)		2.2	2.2	2.2	2.1	2.7	2.9	1.78	2.07	2.37	2.77	2.77

Cladding Metals

Copper Foil	Surface Roughness		Tensile Strength kpsi (MPa)	Elongation %	Volume Resistivity Microhm•cm	Stress Crack Resistance	Thickness mil	Peel Strength RT/duroid 5000 Series lbs/in (KN/m)
	Treated Side	Untreated Side						
1 1/2 oz (9µm) ED	70 (1.8)	15 (0.4)	—	—	1.87	Fair	0.4	11 (1.93)
1 2 oz (17.5µm) ED	75 (1.9)	15 (0.4)	33.0 (228)	20.0	1.82	Fair	0.7	12 (2.10)
1 oz (35µm) ED	95 (2.4)	15 (0.4)	30.0 (207)	28.0	1.78	Fair	1.4	16 (2.80)
2 oz (70µm) ED	115 (2.9)	15 (0.4)	32.0 (221)	42.0	1.78	Fair	2.8	18 (3.15)
1 2 oz (17.5µm) Rolled	55 (1.4)	12 (0.3)	20.0 (138)	8.0	1.78	Excellent	0.7	9 (1.58)
1 oz (35µm) Rolled	55 (1.4)	12 (0.3)	22.0 (152)	13.0	1.74	Excellent	1.4	10 (1.75)
2 oz (70µm) Rolled	55 (1.4)	12 (0.3)	28.0 (193)	27.0	1.74	Excellent	2.8	11 (1.93)

Plates	Alloy	Surface Roughness µin (µm)	Machinability	Tensile Strength kpsi (MPa)	Specific Gravity	Thermal Conductivity W/m ² /°K	Coefficient of Thermal Expansion ppm/°C	Resistivity microhm cm
Aluminum	6061	70 (1.8)	Poor	20 (138)	2.7	180	24	5
Brass	70/30 cartridge	70 (1.8)	Good	45 (311)	8.5	120	20	6
Copper	110	70 (1.8)	Fair to Poor	35 (242)	8.9	390	17	2



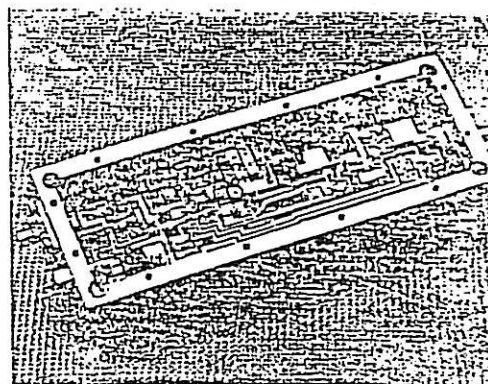
ROGERS

FULL FAMILY

HIGH QUALITY

MICROWAVE

LAMINATES



Now available from **ROGERS** is a full family of high quality microwave laminates.

RT/duroid® 5870 and 5880 substrates, composed of uniformly dispersed glass microfibres in a PTFE matrix, providing the microwave engineer with a microscopically controlled uniform dielectric constant (dk).

RT/duroid® 6002, glass microfibre and ceramic reinforced PTFE laminates, combining excellent plated-through-hole and surface mounting reliability with extremely low variation of dielectric constant in function of temperature.

RT/duroid® 6006 and 6010 substrates, composed of uniformly dispersed ceramic filler in PTFE matrix.

ULTRALAM™ 2000 woven glass reinforced PTFE for improved dimensional stability.

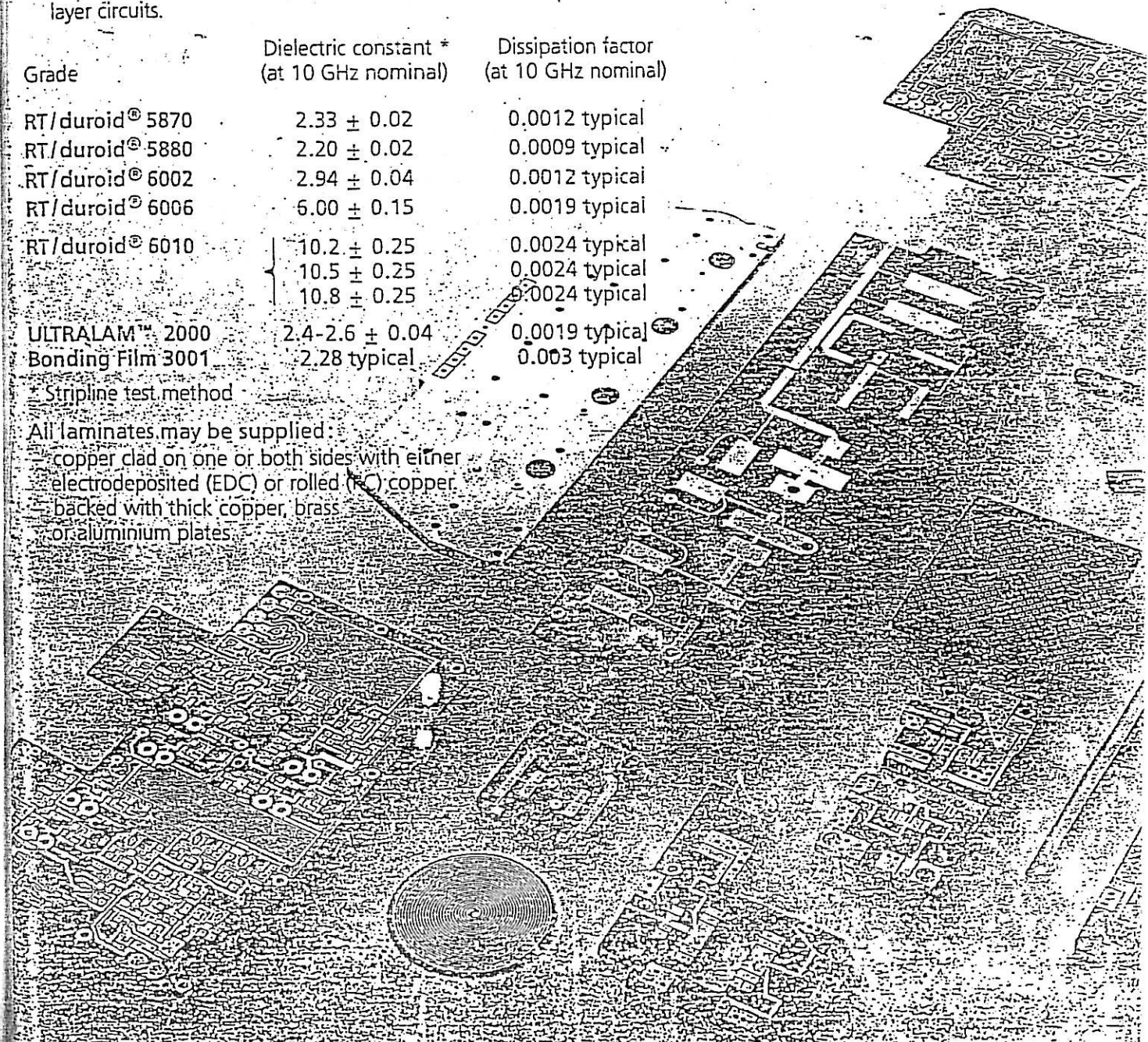
ROGERS™ 3001 Bonding Film, for bonding low dielectric constant PTFE microwave stripline packages and other multi-layer circuits.

Grade	Dielectric constant * (at 10 GHz nominal)	Dissipation factor (at 10 GHz nominal)
RT/duroid® 5870	2.33 ± 0.02	0.0012 typical
RT/duroid® 5880	2.20 ± 0.02	0.0009 typical
RT/duroid® 6002	2.94 ± 0.04	0.0012 typical
RT/duroid® 6006	6.00 ± 0.15	0.0019 typical
RT/duroid® 6010	10.2 ± 0.25	0.0024 typical
	10.5 ± 0.25	0.0024 typical
	10.8 ± 0.25	0.0024 typical
ULTRALAM™ 2000	$2.4-2.6 \pm 0.04$	0.0019 typical
Bonding Film 3001	2.28 typical	0.003 typical

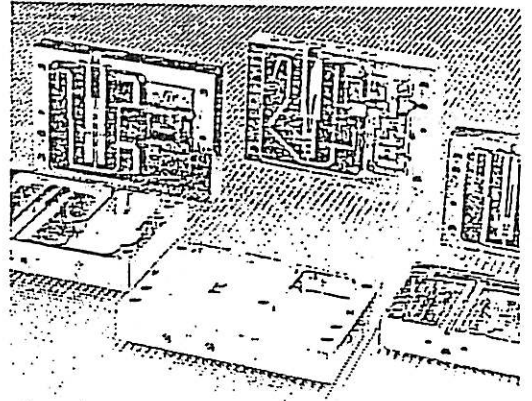
* Stripline test method

All laminates may be supplied:

- copper clad on one or both sides with either electrodeposited (EDC) or rolled (RC) copper.
- backed with thick copper, brass or aluminium plates.



FEATURES



RT/duroid® 5870-5880

- Tight tolerance of dielectric constant and dielectric thickness.
- Excellent machining capabilities.
- High peel strength of copper foil to substrate.
- Very low water absorption, typically less than 0.02 %.
- Low outgassing properties.
- Exceed the requirements of MIL - P - 13949G.

RT/duroid® 6002

- Zero temperature coefficient of dielectric constant.
- Excellent through hole plating reliability.
- Very high surface mount reliability.

RT/duroid® 6006-6010

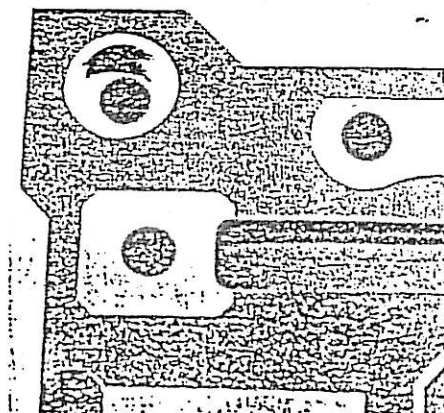
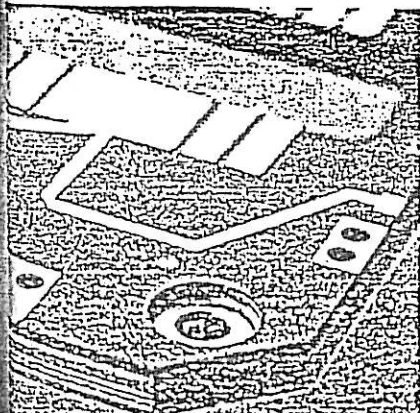
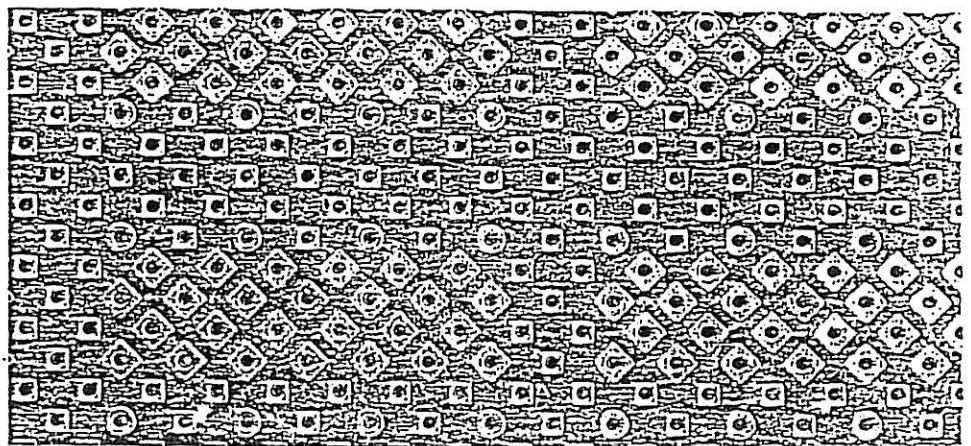
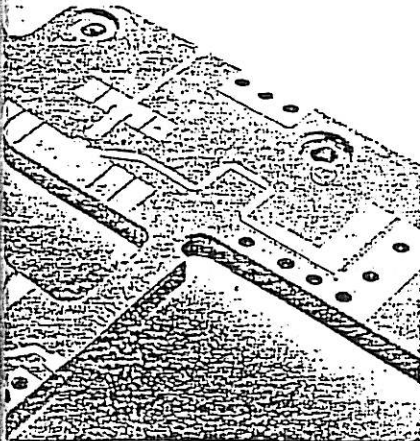
- Ease of fabrication.
- Low moisture absorption.
- Nearly isotropic electrical properties.
- Low strain relief after etching.

ULTRALAM™ 2000

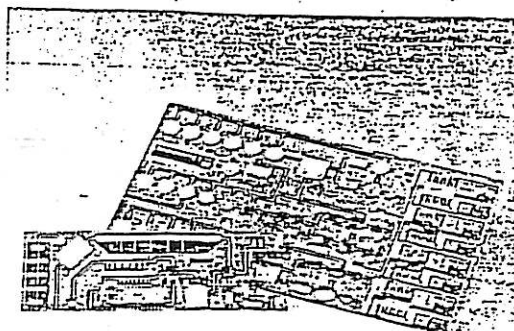
- Excellent mechanical stability.
- Low tolerance on dielectric constant.
- High copper peel strength.

Rogers™ 3001 Bonding Film

- High temperature-resistance.
- Chemically inert.
- Low moisture absorption, typical 0.05 %.



PROPERTIES



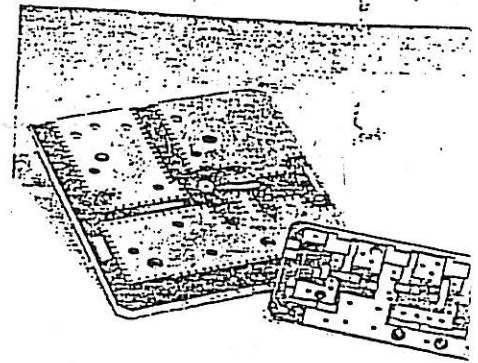
DIELECTRICS

PROPERTY		RT/duroid 5870	RT/duroid 5880	RT/duroid 6002	RT/duroid 6006	RT/duroid 6010	RT/duroid 6010	RT/duroid 6010	ULTRALAM 2000
Dielectric constant and tolerance @ 10 GHz		2.33 ± 0.02	2.20 ± 0.02	2.94 ± 0.04	6.0 ± 0.15	10.2 ± 0.25	10.5 ± 0.25	10.8 ± 0.25	$2.4-2.6 \pm 0.04$
Loss tangent @ 10 GHz		0.0012	0.0009	0.0012	0.0019	0.0024	0.0024	0.0024	0.0019
Thermal coeff. of ϵ_r 0° to 100° (ppm/K)		-115	-129	~0	-350	-390	-390	-390	-100
Volume resistivity (Mohm • cm)		2×10^7	2×10^7	10^6	2×10^7	5×10^5	5×10^5	5×10^5	2×10^7
Surface resistivity (Mohm)		3×10^8	3×10^8	10^7	7×10^7	5×10^6	5×10^6	5×10^6	4×10^7
Tensile modulus (MPa)	X AXIS	1304	1076	828	511	932	932	932	11730
	Y AXIS	1277	853	828	628	559	559	559	8970
Compressive modulus z axis (MPa)		828	938	-	1070	2146	2146	2146	-
Moisture absorption D 23/24 (%)		0.015	0.015	0.1	0.05	0.1	0.1	0.1	0.02
Thermal conductivity (W/m/K)		0.26	0.26	0.44	0.48	0.41	0.41	0.41	0.26
Coefficient of thermal expansion 0° to 100° C (ppm/K)	X AXIS	22	31	16	38	24	24	24	15
	Y AXIS	28	48	16	42	24	24	24	15
	Z AXIS	173	237	24	71	24	24	24	200

This table is designed to help you choose the ROGERS material best suited to your application.

Includes information on RT/duroid® microwave laminates and ULTRALAM™ woven glass/PTEE laminates, which are designed for demanding stripline and microstrip applications.

METALS

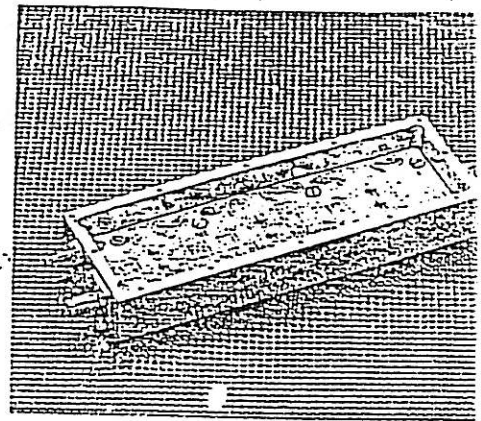


CLADDING METALS

FOILS		Surface roughness (μm)		Tensile strength (MPa)	Elongation (%)	Volume resistivity (microhm • cm)	Stress Crack resistance	Peel strength RT/dioid 5000 Series (N/cm)	
		Treated side	Untreated side						
C O P P E R	5 μm ED (1/8 oz)	1.8	0.4	--	--	1.95	Fair	19	
	9 μm ED (1/4 oz)	1.8	0.4	--	--	1.87	Fair	19	
	17.5 μm ED (1/2 oz)	1.9	0.4	207	25	1.82	Fair	21	
	35 μm ED (1 oz)	2.4	0.4	228	30	1.78	Fair	28	
	70 μm ED (2 oz)	2.9	0.4	228	30	1.78	Fair	32	
	17.5 μm Rolled (1/2 oz)	1.4	0.3	235	40	1.78	Excellent	16	
	35 μm Rolled (1 oz)	1.4	0.3	242	45	1.74	Excellent	18	
	70 μm Rolled (2 oz)	1.4	0.3	242	45	1.74	Excellent	19	
OHMEGA-PLY® (25 ohms/sq.)	Copper (35 μm ED)	--	0.4	228	30	1.78	Fair	--	
	Resistive layer	2.4	--	--	--	1000	Poor	23	
PLATES		Alloy	Surface roughness (μm)	Machinability	Tensile strength (MPa)	Specific gravity	Thermal conductivity (W/m/K)	Coeff. of therm. expan. (ppm/K)	Resistivity (microhm • cm)
Aluminium		6061	1.8	Poor	138	2.7	180	24	5
Brass		70/30 cartridge	1.8	Good	311	8.5	120	20	11
Copper		110	1.8	Fair to Poor	242	8.9	390	17	2
Copper/Invar®/Copper		20 % Cu 60 % Fe/Ni 20 % Cu	1.8	Good	414	8.4	~35	5	4

Note: Typical values shown on all tables unless tolerances are given.

AVAILABILITY



RT/duroid® 5870 and 5880

DIELECTRIC CONSTANT

RT/D 5870: $\epsilon_r = 2.33 \pm 0.02$

RT/D 5880: $\epsilon_r = 2.20 \pm 0.02$

Specification MIL-P-13949G type GRN

CLADDING

COPPER: 5 μ m ED Copper (1/8 oz)
 9 μ m ED Copper (1/4 oz)
 17.5 μ m Rolled or ED Copper (1/2 oz)
 35 μ m Rolled or ED Copper (1 oz)
 70 μ m Rolled or ED Copper (2 oz)

On special request we can supply Aluminium, Brass or Copper backed material and Ohmega - ply.

SHEET SIZE AND THICKNESS

Size:	inches	mm
	18 x 12	457 x 305
	18 x 24	457 x 610
	18 x 36	457 x 915
	18 x 48	457 x 1219

Thickness and tolerance:

0,005 \pm 10 %	0,13 \pm 10 %
0,010 \pm 7 %	0,25 \pm 7 %
0,015 \pm 7 %	0,38 \pm 7 %
0,020 \pm 0,001	0,51 \pm 0,03
0,031 \pm 0,001	0,79 \pm 0,03
0,062 \pm 0,002	1,57 \pm 0,05
0,125 \pm 0,004	3,18 \pm 0,10

Other sheetsizes and thicknesses available on request.

RT/duroid® 6002

DIELECTRIC CONSTANT

RT/D 6002: $\epsilon_r = 2.94 \pm 0.04$

CLADDING

COPPER: 5 μ m ED Copper (1/8 oz)
 9 μ m ED Copper (1/4 oz)
 17.5 μ m Rolled or ED Copper (1/2 oz)
 35 μ m Rolled or ED Copper (1 oz)
 70 μ m Rolled or ED Copper (2 oz)

On special request we can supply Aluminium, Brass or Copper backed material and Ohmega - ply.

SHEET SIZE AND THICKNESS

Size:	inches	mm
	18 x 12	457 x 305
	18 x 18	457 x 457
	18 x 24	457 x 610

Thickness and tolerance:

0,005 \pm 10 %	0,13 \pm 10 %
0,010 \pm 7 %	0,25 \pm 7 %
0,020 \pm 0,001	0,51 \pm 0,03
0,030 \pm 0,001	0,76 \pm 0,03
0,060 \pm 0,002	1,52 \pm 0,05

Other sheetsizes and thicknesses available on request.

RT/duroid® 6006 and 6010

DIELECTRIC CONSTANT

RT/D 6006: $\epsilon_r = 6.00 \pm 0.15$

RT/D 6010: $\epsilon_r = 10.2 \pm 0.25$

RT/D 6010: $\epsilon_r = 10.5 \pm 0.25$

RT/D 6010: $\epsilon_r = 10.8 \pm 0.25$

CLADDING

COPPER: 5 μ m ED Copper (1/8 oz)
 9 μ m ED Copper (1/4 oz)
 17.5 μ m Rolled or ED Copper (1/2 oz)
 35 μ m Rolled or ED Copper (1 oz)
 70 μ m Rolled or ED Copper (2 oz)

On special request we can supply Aluminium, Brass or Copper backed material and Ohmega - ply.

SHEET SIZE AND THICKNESS

Size:	inches	mm
	20 x 20	508 x 508
	10 x 20	254 x 508
	10 x 10	254 x 254

Thickness and tolerance:

0,010 \pm 0,001	0,25 \pm 0,03
0,025 \pm 0,001	0,64 \pm 0,03
0,050 \pm 0,002	1,27 \pm 0,05
0,075 \pm 0,004	1,91 \pm 0,10
0,100 \pm 0,005	2,54 \pm 0,13

Other sheetsizes and thicknesses available on request.



ROGERS FULL FAMILY HIGH QUALITY MICROWAVE LAMINATES

ULTRALAM™ 2000

DIELECTRIC CONSTANT

ULTRALAM™ 2000: $\epsilon_r = 2.4 - 2.6 \pm 0.04$

Dielectric: 0.0040 ± 0.0004 $\epsilon_r = 2.40$

thickness: 0.0101 ± 0.0009 $\epsilon_r = 2.48$

0.0147 ± 0.001 $\epsilon_r = 2.45$

0.0190 ± 0.001 $\epsilon_r = 2.43$

0.0300 ± 0.001 $\epsilon_r = 2.4 - 2.6$

0.0600 ± 0.002 with 0.05 increments

CLADDING

COPPER:

5 μ m ED Copper (1/8 oz)

9 μ m ED Copper (1/4 oz)

17.5 μ m Rolled or ED Copper (1/2 oz)

35 μ m Rolled or ED Copper (1 oz)

70 μ m Rolled or ED Copper (2 oz)

On special request we can supply Aluminium, Brass or Copper backed material and Ohmega - ply.

SHEET SIZE AND THICKNESS

Size:	inches	mm
	18 x 12	457 x 305
	18 x 24	457 x 610
	18 x 48	457 x 1219

Thickness and tolerance:

0.0040 ± 0.0004	$0.10 \pm 10\%$
0.0101 ± 0.0009	0.25 ± 0.02
0.0147 ± 0.001	0.37 ± 0.03
0.0190 ± 0.001	0.48 ± 0.03
0.0300 ± 0.001	0.76 ± 0.03
0.0600 ± 0.002	1.52 ± 0.05

Othersheet sizes and thicknesses available on request.

ROGERS™ 3001 Bonding Film

Dielectric constant: $\epsilon_r = 2.28$

Film thickness: 38 μ m (0.0015")

Standard rolls: 305 mm wide (12") x 15.2 m long (50 ft.)

AGENT



MAIN SUBSIDIARIES

ROGERS

AMERICA, U.S.A.

Mektron N.V.

European

Headquarters

Afrikalaan 188

B-9000 GENT

BELGIUM

Tel.: (091) 35 36 11

Telex: 11 553

Fax: (091) 35 36 58

Mektron-France S.A.

2, Place de l'Equerre

SILIC 307

F-94588 RUNGIS CEDEX

FRANCE

Tél.: (1) 46 87 22 70

Télex: 260 719

Fax: (1) 46 87 66 90

Mektron Circuit
Systems Ltd.

119, Kingston Road

LEATHERHEAD

SURREY KT 22 7SU

UNITED KINGDOM

Tel.: (03723) 78233

Telex: 928674

Fax: (03723) 75888

Mektron GmbH

Eschenweg 2-4

D-6108 WEITERSTADT

W.-GERMANY

Tel.: (06150) 14081

Telex: 4197223

Fax: (06150) 12254

DESIGN OF MICROSTRIP BAND PASS FILTER AT 2 GHz

M.K. Abdul Rahim & M. B. Shamsuddin
Department of Radio Communication Engineering
Faculty of Electrical Engineering
Universiti Teknologi Malaysia
Skudai Johor
Malaysia

Fax : 60 7 5566272
mkamal@suria.fke.utm.my

Abstract

This paper is concerned with designing a bandpass filter to be used in microwave communication transceiver. The filter configuration chosen is based on microstrip planar resonators for the operation from 1.9 to 2.1 GHz. The procedures presented here are applicable for the design of a parallel coupled bandpass filter. The major design process is aided by CAD package called PUFF. Different configuration of resonators with various parameters governing the performance of the filter are investigated using the simulation model. The results of the simulations are presented here. The best choice of the microwave bandpass filter configurations are recommended

Introduction

Bandpass filters require precise transmission characteristic that allows a desired band of signals to pass through the two port network. Thus between transmitter and receiver, a band pass filter is used to attenuate unwanted signals. There are two basic forms of coupled resonator bandpass filters in microstrip line. The first form is an end coupled filter which has a capacitive coupling from each end of the resonator into the end of the adjacent line. On the other hand, edge or parallel coupled filters have resonators that are coupled through the even and odd mode fields along the edges of the lines. Parallel coupled filters are generally preferred because they lead to as much as 50% reduction in length. Furthermore larger gaps between the lines are permitted for parallel coupled filters easing the tolerances and permitting a broader bandwidth for a given dimensional tolerance. The greatest significance is that the first spurious response for a parallel coupled filter occurs a three times the center frequency of the filter whereas the end coupled occurs only twice.

Design Consideration

Parallel coupled lines are used for the band pass filter design. For coupled lines maximum coupling is obtained when the length of the coupled region is $\lambda_g/4$. To achieve resonance, each resonator elements has to be $\lambda_g/2$ in length. Figure 1 shows the parallel coupling method which will be used in this design. The first coupling structure is formed by w_1, s_1, w_1 and the final coupling structure is also consists of s_1, w_1, s_1 at the opposite end of the filter.

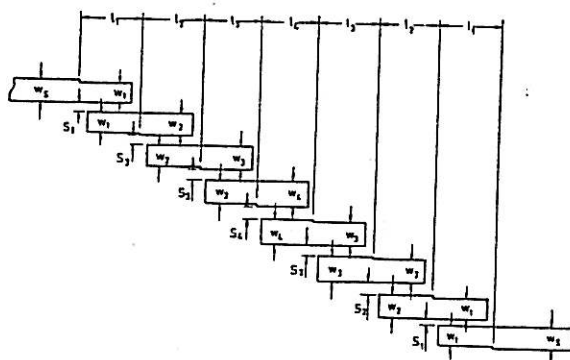


Figure 1 : Parallel coupled bandpass filter for seven section configuration

The main design step are as follows

- Mapping from low pass prototype to band pass

Designing process starts with the transformation of low pass prototype into band pass requirements. The purpose of this idea is to determined the number of resonators that is

needed to meet the attenuation requirement. This is to determine the order of the filter. The mapping of low pass prototype into bandpass is done by using this equation

$$\frac{\omega_i}{\omega_c} = \frac{2}{\Delta f} \left(\frac{f_i - f_0}{f_0} \right)$$

where $\Delta f = \frac{f_2 - f_1}{f_0}$

Δf = fractional bandwidth

f_1 = lower pass band

f_2 = upper pass band

f_0 = center frequency

ω_c = prototype cut off frequency (equals to 1)

ω_i = defined in filter specification

f_i = frequency at desired attenuation

- Determine the number of resonators that is the order of the filter

Determine the order of the filter that is the value for n by examining the filter prototype specifications which meet the insertion loss requirements, that is should be at least 20 dB (desired attenuation) for the desired frequency in the design specifications. For n th order of filter there will be $n + 1$ number of resonators (coupled region). The order of the filter is determined by referring the graph for Chebyshev characteristic for 0.01 ripple.

- Calculate the admittance inverters values

A network consisting of admittance inverters and uniform type resonant circuits were used. The admittance inverter parameters are then calculated

For the first coupling structure

$$\frac{J_{01}}{Y_0} = \sqrt{\frac{\pi \Delta f}{2 g_0 g_1}}$$

For intermediate coupling structures

$$\left. \frac{J_{j,j+1}}{Y_0} \right|_{j=1 \text{ to } (n-1)} = \frac{\pi \Delta f}{2 \omega_c' \sqrt{g_j g_{j+1}}}$$

For the final coupling structure

$$\frac{J_{n,n+1}}{Y_0} = \sqrt{\frac{\pi \Delta f}{2 g_n g_{n+1}}}$$

The quantities g refer to the prototype elements value which is readily available from the table provided [1]. The value for g is selected according to the order (n) of the filter.

- Evaluate the even and odd mode characteristic impedance (Z_{0e} and Z_{0o})

The odd mode and even mode coupled line impedance Z_{0o} and Z_{0e} are then calculated by using this equation [1]

$$(Z_{0e})_{j,j+1} = Z_0 (1 + aZ_0 + a^2 Z_0^2)$$

$$(Z_{0o})_{j,j+1} = Z_0 (1 - aZ_0 + a^2 Z_0^2)$$

where $a = J_{j,j+1}$

Z_0 = system characteristic impedance

- Calculate the resonator length

The length of resonator l is calculated by using equation given below where we have to evaluate the physical length of the resonator $\lambda_g/2$ and the physical value of coupled region $\lambda_g/4$

where $\lambda_g = \frac{300}{f \sqrt{\epsilon_{eff}}} \text{ mm}$

f = operating frequency in GHz

ϵ_{eff} = effective permittivity

Simulation

The design process is further continued with the utilization of the PUFF simulation. From the result of the simulation, the response of the band pass filter can be visualized. The design is analyzed according to the S parameter obtained from the simulation. The simulation process started with the calculated values. Then the simulations for the purpose of optimization are done by doing some adjustment to the length of the resonators and increasing the order of the filters.

The simulation result can be shown as in figure 2 to 6 with different order of the filters.

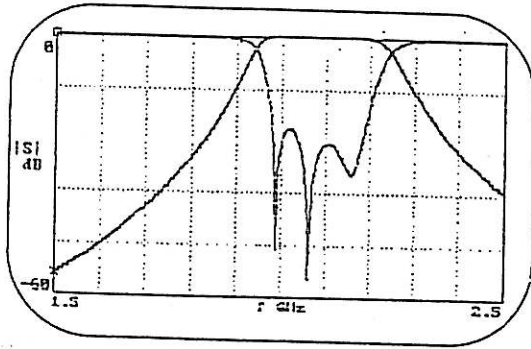


Figure 2: Simulation for 4th order bandpass filter with five coupled sections of resonators

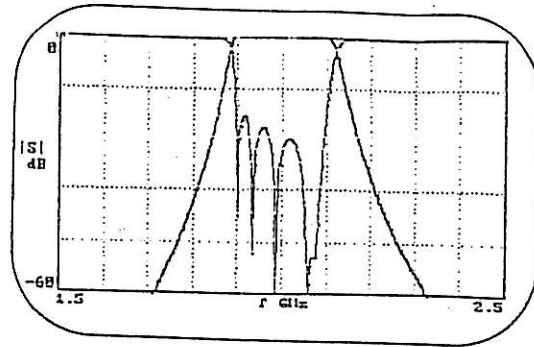


Figure 5 : Simulation for 6th order with seven section of resonator

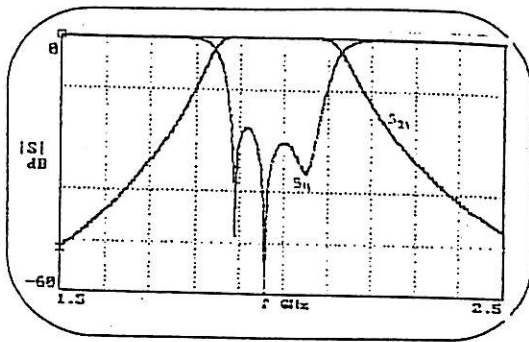


Figure 3 : Simulation for 4th order filter with different length of coupled region

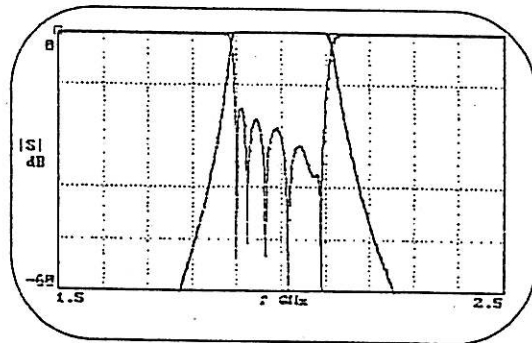


Figure 6 : Simulation for 7th order with 8 sections of resonators

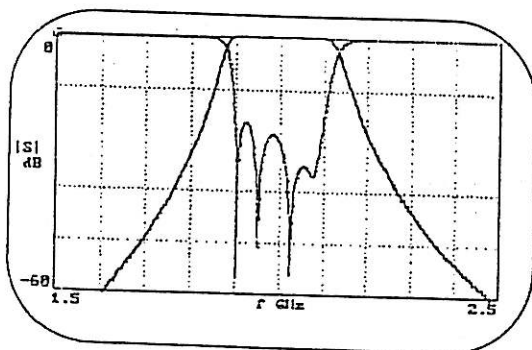


Figure 4 : Simulation for 5th order with six sections of resonator

Discussion

The simulation result for the actual calculated values show the design still needs a lot of optimization because the error is very high. It was found out that the bandwidth error is 51.8%. The first optimization is done by increasing the resonators length i.e. figure 3. The order of the filter is still the same. However this is the best result that can be obtained by varying the resonator length. The bandwidth error is 43.7% and this still considered high. So further optimization is done by increasing the order of the filter.

From the overall simulation results, it was found out that the simulations in figure 6 is the best for the filter design. This is 7th order filter. The bandwidth error is 8.9% and the center frequency error is 0.075%. the desired 20 dB attenuation at the early design stage is 1.7 GHz, but the value obtained is at 1.8667 GHz. This is acceptable

because we need at least 20 dB attenuation at 1.7 GHz

Conclusion

The design process of the band pass filter is based on the S parameter from the PUFF simulation. We are only concern about S_{11} (return loss) and S_{21} (insertion loss). The basic concept is in the pass band of the filter, the S_{11} value should be kept as low as possible meanwhile the value of S_{21} should be kept at 0 dB.

In order to achieve the best result optimization was done. During the optimization process the analysis of the bandwidth and the center frequency were given more priority. It is realized that while doing optimization certain error of parameters have to be sacrifice to maintain the minimum error in the bandwidth with the center frequency. From the overall result of simulation it was notified that the operating frequency can be shifted by varying the resonator length. It was found out that operating frequency is shifted to the left when the resonator length is increased. Furthermore the result also prove that the cut of response is sharper for the higher order filters. Besides the higher order filter is found to have narrower bandwidth compared to the lower order filters. The optimization process was carried out based on these above mentioned criteria

Reference

- [1] Terry Edwards., 'Foundations for microstrip design', 2nd edition, John Wiley and sons 1995
- [2] Akhtarzad, S., Rowbotham, T.R., Jones, P.B., 'The design of coupled microstrip lines'. IEEE Trans MTT-23 No 6 June 1975
- [3] E. H. Fooks, R. A. Zakrevicous, 'Microwave Engineering Using Microstrip Circuits, Prentice Hall, 1990
- [4] Dydyk, M., 'Accurate design of microstrip directional couplers with capacitive compensation', IEEE MTT-S International Microwave Symposium 1990.
- [5] Kajfez, D., and Govind, S., 'Effects of difference in odd and even mode wavelength on a parallel coupled bandpass filter', Electron.Lett., March 1975.
- [6] Matthaei, G.L., Young, L., and Jones, E.M.T., Microwave Filters, Impedance - Matching Networks and Coupling Structures, Mc Graw Hill, New York 1965